Planetary, Solar, Radio and Heliospheric Radio Emissions (PRE) IX Conference Dublin, Ireland, 2022 September 26th - 28th

DIAS

Institiúid Ard-Léinn Bhaile Átha Cliath | Dublin Institute for Advanced Studies

This is the 2022, September 13th version of the PRE IX program

Contents

About

Planetary, Solar and Heliospheric Radio Emission (PRE) Conference Series

The 9th International Workshop on "Planetary, Solar and Heliospheric Radio Emissions" is the continuation of an established tradition following previous successful international workshops held in Austria, in 1984, 1987, 1991, 1996, 2001, 2005, 2010, and 2016. Proceedings of these previous PRE conferences can be found open access at austriaca.at/pre.

We expect this workshop to follow a hybrid format, with all talks live streamed online via a communication platform that will allow questions from both in-person and virtual audiences. There will be poster lightning talks to accommodate both audiences, and posters will also be able to be displayed at the venue for in-person attendees.

For this edition, we also plan to publish a PRE IX conference proceedings book.

Scientific Organising Committee

Caitriona Jackman
Georg Fischer
Laurent Lamy
Hamish Reid
Pietro Zucca

Local Organising Committee

Eoin Carley
Eileen Flood
Alexandra Fogg
Peter Gallagher
Caitriona Jackman
Corentin Louis
Sophie Murray
Elizabeth O'Dwyer
James Waters

Practical Information

Venue

The conference will be held at [Clayton Cardiff Lane](#) in the heart of Dublin City Centre near the Docklands. The hotel has a brand new conference facility with state-of-the-art technology to accommodate hybrid meetings.

Address: Clayton Hotel Cardiff Lane, Sir John Rogerson's Quay, Dublin Docklands, Dublin, D02 YT21

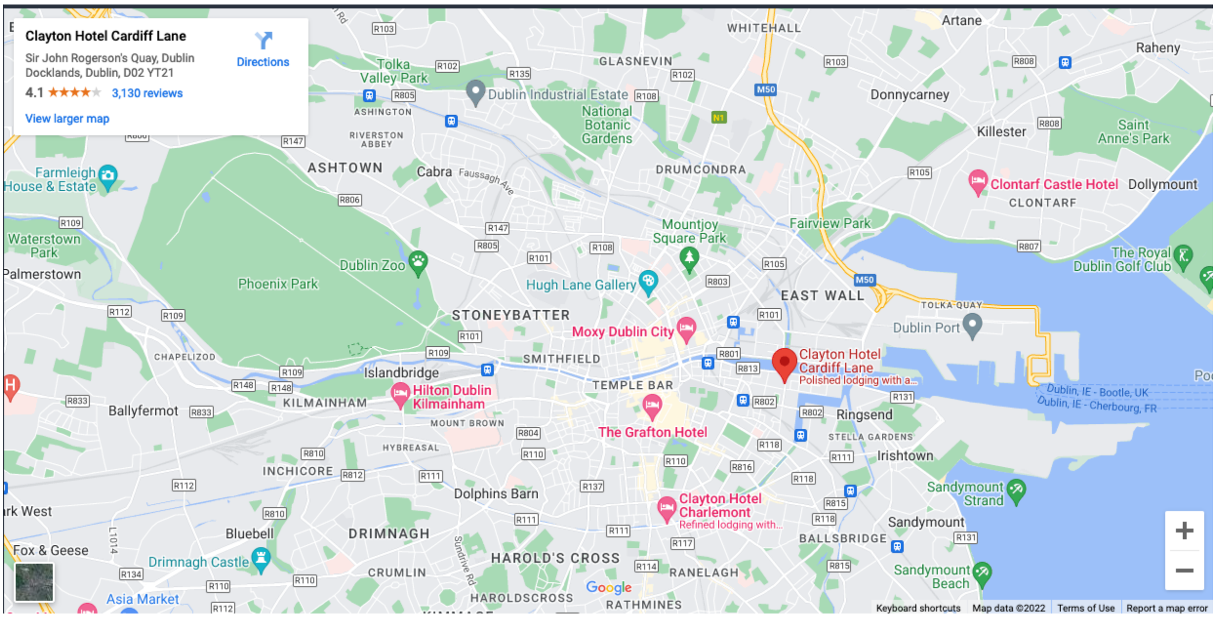

The venue is 12km from Dublin Airport, a 20 – 30 minute taxi or bus ride away depending on traffic! Taxis are available at the stands outside arrival areas of both terminals, expect it to cost ~ €30. [Aircoach Route 702](#) stops right outside the venue and costs €8 one-way. Alternatively [Dublin Bus](#) (cheaper but slower!) Numbers 16 and 41 go from the airport into the city centre.

The PRE 2022 conference venue is a short walk away from most major attractions. [Dublin City Bikes](#) are also available to hire from many locations across the city. A three-day subscription costs €5, with the first 30 minutes free for any journey before rental charges apply.

To explore Dublin's surrounding areas the hotel is close to numerous Dublin Bus stops, 5 minutes walk from the Spencer Dock tram stop (on the Luas Red Line), and 10 minutes walk to Pearse Street train station.

Accommodation

A rate of €235 single bed and breakfast or €250 double/twin bed and breakfast per night is available at the Clayton Hotel Cardiff Lane – book with the hotel directly. There are also many hotels in Grand Canal Dock, Dublin City Centre, and surrounding areas that are all a short walk away from the venue.

Registration

Costs for registration are: €220 for normal delegates, €150 for students, and €60 for online attendance. The in-person registration fees cover tea/coffee and lunches for 3 days, as well as the conference dinner on Tuesday night.

The in-person registration does not include the Thursday I-LOFAR tour. This extra cost will be defined later.

Conference Dinner

We will hold a conference dinner on Tuesday September 27th at the Old Storehouse pub, within easy walking distance of the daytime conference venue. Costs for attendance at conference dinner will be included in the registration fee. More information about the dinner venue at pre2022.dias.ie/conference-dinner.

I-LOFAR tour

An (optional) excursion at Birr Castle to visit the Irish-LOFAR (LOw Frequency ARray) radiotelescope will be organized on Thursday, September 29th.

Talks and posters

The contributed talks will be 15 minutes long (12 minutes + questions) and the invited talks will be 30 minutes long (25 minutes + questions.)

Poster boards will be 1 m x 1m in dimension, thus we recommend A0 portrait and A1 landscape format. Please note that we do not have access to poster printing facilities, it is up to attendees to print posters themselves before the meeting

For more information and updates, please visit our website (https://pre2022.dias.ie/)

Talks will be diffused online, as well as the lightning poster. Poster session won't be distributed online.

Schedule

Monday, September, 26th

Session 1	**09:00 - 10:45**	**Planetary - Jupiter**		**Eligible for student presentation prize**
Chair	**Philippe Zarka**			
	09:00 - 09:15	**SOC/LOC [Jackman]**	**Welcome and setup. Code of conduct, breaks, wifi, dinner**	
	09:15 - 09:45	Imai - invited [30 min]	High-resolution observations of Jupiter's auroral radio emissions from Juno	
	09:45 - 10:00	Bolton	Juno Observations of Jupiter's Synchrotron Emission and Radiation Belts	
	10:00 - 10:15	Boudouma	Large scale numerical modeling of the jovian plasma emissions with Juno	X
	10:15 - 10:30	Louis	Effect of magnetospheric disturbances on Jovian radio emissions: an in situ case study from Juno data	
online	10:30 - 10:45	Kharlanova	Ground support of Juno mission and data preprocessing	X
Break	**10:45 - 11:15**			
Session 2	**11:15 - 12:30**	**Planetary - Jupiter**		
Chair	**Corentin Louis**			
	11:15 - 11:30	Sulaiman	Electron densities in Jupiter's polar regions: Implications for the generation of auroral and radio emissions	
	11:30 - 11:45	Collet	Characterization of jovian decametric auroral emissions (DAM) using in situ radio and electron data	X
	11:45 - 12:00	Lamy	Determining the beaming of Io decametric emissions : a remote diagnostic to probe the Io-Jupiter interaction	
online	12:00 - 12:15	Zheng	Statistical Study on the Jovian Decametric Radio Emissions Based on Multiple-view Observations from Remote Radio Instruments	X
	12:15 - 12:30	Don Gurnett tribute [Bill Kurth, George Hospodarsky]	Don Gurnett Tribute	
Lunch	**12:30 - 14:00**	**Lunch**		
Session 3	**14:00 - 15:30**	**Planetary - Lightning + AKR**		
Chair	**Joe Kinrade**			
	14:00 - 14:15	Kolmasova	New insights into Jovian lightning thanks to high-resolution electromagnetic measurements onboard Juno	
	14:15 - 14:30	Santolik	Propagation of radio waves from lightning discharges through the Jovian ionosphere	
online	14:30 - 14:45	Hospodarsky	Jupiter Long Dispersion Lightning Whistlers associated with the Io torus: Juno Observations	
	14:45 - 15:00	LaBelle	Advances in leaked Auroral Kilometric Radiation	
	15:00 - 15:15	Taubenschuss	Classification of the spectral fine structure in Auroral Kilometric Radiation	
	15:15 - 15:30	Waters	Novel Wind/Waves AKR Observations and Use in Exploring Magnetospheric Dynamics	X
Break	**15:30 - 16:00**			
Session 4	**16:00 - 17:30**	**POSTERS**		
Chair	**Caitriona Jackman**			
	16:00 - 16:30	ALL POSTER AUTHORS	1 MINUTE LIGHTNING TALKS TO INTRODUCE POSTERS	
	16:30 - 17:30	**POSTERS**	**POSTERS**	

Tuesday September 27th

Session 5	09:00 - 10:45	Solar		Eligible for student presentation prize
Chair	Diana Morosan			
online	09:00 - 09:30	Mohan - invited [30 min]	Insights on solar-stellar atmospheric activity from modern sensitive radio and mm-arrays.	
online	09:30 - 09:45	Chen	The frequency ratio and time delay for solar radio emissions with fundamental and harmonic components	
	09:45 - 10:00	Clarkson	Radio-wave Scattering Effects on Observations of Solar Radio Spikes and Type IIIb Striae Within a Closed Loop System	X
	10:00 -10:15	Koval	Meter-decameter observations of "fractured" type II solar radio bursts	
	10:15 - 10:30	Kumari	On the source sizes of fine structures of type II radio bursts using LOFAR	
	10:30 - 10:45	Benáček	Double plasma resonance model of solar radio zebras	
Break	**10:45 - 11:15**			
Session 6	**11:15 - 12:45**	**Solar ground-based**		
Chair	**Pietro Zucca**			
online	11:15 - 11:30	Dey	First detailed polarimetric study of a group of type III solar radio bursts with the Murchison Widefield Array	X
online	11:30 - 11:45	Kansabanik	Coronal Magnetic Field Measurement during Quiet Time using Low-Frequency Spectropolarimetric Imaging	X
	11:45 - 12:00	Kozarev	Observations and Modeling of The Quiet Solar Corona in Low Frequency Imaging	
	12:00 - 12:15	Murphy	Automatic detection of radio bursts in NenuFAR solar observations	
	12:15 - 12:30	Morosan	The escape and propagation of shock-accelerated electron beams during a solar coronal mass ejection	
	12:30 - 12:45	**ALL**	**GROUP PHOTO**	
Lunch	**12:45 - 14:00**	**Lunch**		
Session 7	**14:00 - 15:30**	**Solar space-based**		
Chair	**Peter Gallagher**			
	14:00 - 14:30	Bale - invited [30 min]	Low-frequency solar radio astronomy in the era of Parker Solar Probe and Solar Orbiter	
	14:30 - 14:45	Nedal	Simultaneous Observations of Solar Radio Bursts using LOFAR and Spacecraft Instruments	X
	14:45 - 15:00	Krupar	Type III Bursts and Solar Energetic Particles	
	15:00 - 15:15	Rigney	Low Frequency Radio Emission Associated with an Impulsive Flare and Coronal Mass Ejection	X
	15:15 - 15:30	Zhang	Offset Measure: Quasars as detector for electron density in solar atmosphere and inner heliosphere	
Break	**15:30 - 16:00**			
Session 8	**16:00 - 18:00**	**Space Weather + POSTERS**		
Chair	**Pearse Murphy**			
online	16:00 - 16:30	Klein - invited [30 min]	Radio techniques for Space Weather	
	16:30 - 16:45	Zucca	Incremental Development of LOFAR Space-Weather - IDOLS	
	16:45 - 17:00	Lawrance	A Comprehensive analysis on RSTN metric type II bursts and their association with space weather events in solar cycle 24	
	17:00 - 17:15	Miteva	Recent advances on solar radio burst emissions, eruptive phenomena, and geomagnetic storms associated with in-situ particles in solar cycles 23 and 24	
	17:15 - 18:00	**POSTERS**	**POSTERS**	
	18:45 -	**Conference Dinner at the Old Storehouse Pub**		

Wednesday September 28th

Session 9	09:00 - 10:45	Planetary - Saturn		Eligible for student presentation prize
Chair				
	09:00 - 09:30	Wu - invited [30 min]	Magnetospheric dynamics revealed by the low-frequency radio components at Saturn	X
	09:30 - 09:45	Fischer	A special form of low-frequency cutoff of Saturn kilometric radiation	
	09:45 - 10:00	Jackman	A statistical view of the response of Saturn's radio emissions to solar wind driving	
	10:00 -10:15	Kinrade	Testing the relationship between Saturn's ENA and narrowband SKR emissions	
	10:15 - 10:30	O'Dwyer	Machine Learning for the Classification of Low Frequency Extensions of Saturn Kilometric Radiation	X
	10:30 - 10:45	Pisa	Electron solitary waves observed during the SKR source crossings by the Cassini Wideband receiver	
Break	**10:45 - 11:15**			
Session 10	**11:15 - 12:30**	**Exoplanets**		
Chair				
	11:15 - 11:45	Vedantham - invited [30 min]	Hunting for radio flashes from stars, brown-dwarfs and exoplanets	
	11:45 - 12:00	Zarka	Stellar and exoplanetary radio emissions with LOFAR detected via multi-objects dynamic spectroscopy	
	12:00 - 12:15	Turner	Follow-up observations of the first possible exoplanet radio detection	
	12:15 - 12:30	Grießmeier	Required conditions for an exoplanet to emit radio waves and implications for observational campaigns	
Lunch	**12:30 - 14:00**	**Lunch**		
Session 11	**14:00 - 15:15**	**Exoplanets/interplanetary**		
Chair				
	14:00 - 14:15	Mauduit	Exoplanet radio search with NenuFAR	X
	14:15 - 14:30	Ashtari	Detecting Beamed Radio Emission from Exoplanets	
	14:30 - 14:45	Hiremath	The null detection of exoplanetary radio emission: Role of seed magnetic field structure of primordial origin	
	14:45 - 15:00	Kurth	Plasma Densities Measured in the Very Local Interstellar Medium	
Break	**15:00 - 15:45**			
Session 12	**15:45 - 17:00**	**Instrumentation**		
Chair	**Ulrich Taubenschuss**			
online	15:45 - 16:00	Pellizzoni	Single-Dish Solar Radio Imaging with INAF Radiotelescopes	
online	16:00 - 16:15	Knapp	AERO-VISTA: Vector sensor mapping of the Earth's auroral radio emission with twin 6U CubeSats	
	16:15 - 16:30	Cecconi	TFCat, a Spectro-Temporal Feature Catalogue format	
	16:30 - 16:45	Isham	An Advanced Low-band VHF Radar Observatory for Solar, Space Weather, Planetary, and Astronomical Research	
	16:45 - 17:00	**Jackman**	**Closing remarks, I-LOFAR Thursday trip discussion**	

Thursday September 29th (optional)

Excursion to Birr-Castle to visit the Irish-LOFAR (LOw Frequency ARray) Radiotelescope.

Bus will leave the Clayton hotel Thursday morning at 09:30. 2 hour trip to Birr.
Tea/coffee and tour of science centre on arrival.
Lunch and tour of Leviathan telescope and I-LOFAR before return in afternoon (bus leaving approximately 4pm).

List of Poster presentations

Poster #	Name	Student Y/N	Topic	Title
1	Dabrowski, B	N	solar	Interferometric imaging of the type IIIb and U radio bursts observed with LOFAR
2	Dong, L.	N	solar	A new L-S solar flux radio telescope and its recently observation results
3	Wołowska, A.	N	solar	Fine structure of a solar type III radio bursts observed with LOFAR
4	Briand, C.	N	solar	Solar Radio Observations at high spectral and temporal resolution with NenuFAR
5	Amin, M.	Y	solar	Type III solar radio burst masking using convex hulls and uniform subdivision
6	Bhunia, S.	Y	solar	Imaging-spectroscopy of a band-split type II solar radio burst with the Murchison Widefield Array
7	Essien, P.	N	solar, heliospheric	Ionospheric Plasma Fluctuation RESPONSE to space weather events in September 2017, August 2018 and March 2015 (St Patrick's day) over the Equatorial and Low Latitude ionosphere.
8	Prasannakumara Pillai Geethakumari, G	Y	heliospheric	Total Electron Content Variation during a HSS/CIR driven storm in High and Middle Latitudes
9	Nwankwo, V.	N	heliospheric	Probing the response of the D-region ionosphere to solar flares and associated geomagnetic activity over Ireland
10	Sanchez-Cano , B.	N	solar, heliospheric	Detection of Solar radio bursts at Mars
11	Wu, S.	Y	planetary, heliospheric	Observations of the First Harmonic of Saturn Kilometric Radiation during Cassini's Grand Finale
12	Louis, C.	N	planetary	Radio emissions induced by Uranus-moons interactions?
13	Majid, W.	N	planetary	Radio Emissions from Electrical Activity in Martian Dust Storms
14	Misawa, H.	N	planetary	Reconsideration for causalities of occurrence features of Jupiter's Io-related radio emission
15	Kurth, W.	N	planetary	Evidence of fresh injections related to the interchange instability in the Io torus
16	Peixoto Jácome, H.	Y	planetary	Statistical Analysis of the Jovian Decametric Emissions with the Nançay Decameter Array
17	Fischer, G.	N	planetary	Fine and coarse spectral structures of Jovian kilometric radiation revealed by Juno and Cassini
18	Smith, K.	Y	planetary	Latitudinal Distribution of Auroral Kilometric Radiation based on POLAR spacecraft observations
19	Yasuda, R.	Y	planetary	Numerical radar simulation for the explorations of the ionospheres of Jupiter's icy moons
20	Fogg, A.	N	planetary	Quantification of Magnetosphere - Ionosphere coupling timescales using mutual information: response of terrestrial radio emissions and ionospheric/magnetospheric currents
21	Zie, T.	Y	planetary	Variations of the peak positions in the longitudinal profile of noon -time equatorial electrojet
22	Ó Fionnagáin, D.	N	planetary	Constraints of ground-based detections of Uranian electrostatic discharges
23	Lamy, L.	N	planetary	The peak frequency source of Saturn's Kilometric Radiation
24	Zarka, P.	N	planetary	Jupiter's Auroral Radio Emissions Observed by Cassini: Rotational Versus Solar Wind Control, and Components Identification
25	Zarka, P.	N	planetary	Ubiquitous Jupiter fast drifting radio bursts reveal Alfvénic electron acceleration
26	Zarka, P.	N	instrumentation	NenuFAR, a new low-frequency radiotelescope for studying planetary, solar, exoplanetary and stellar radio emissions
27	Langtry , M.	N	instrumentaion/ outreach	Thunderbolts and Lightning, very very enlightening: Engaging and educating audiences with public displays of a 1 million volt musical Tesla Coil.
28	Kozarev, K.	N	instrumentation	STELLAR: An EU Twinning Project on LOFAR Data Analysis and Knowledge Transfer
29	Higgins, C.	N	instrumentation	The Radio JOVE Project 2.0
30	Bale, S.	N	instrumentation	The Lunar Surface Electromagnetics Experiment: LuSEE 'Night'
31	Canizares, A.	Y	solar, instrumentation	SURROUND, A constellation of CubeSats around the Sun
32	Cecconi, B.	N	instrumentation	A consolidated catalogue of Jovian decametric radio emissions observed in Nançay from January 1978 to 1990
33	Lamy, L.	N	instrumentation	Daily observations of Jupiter and the Sun with the Nançay Decameter Array : long-term monitoring and support to space missions
34	Lamy, L.	N	instrumentation	Re-exploring the radio spectrum of Uranus with a novel orbital mission : science case and digital instrumentation
35	Lamy, L	N	exoplanets	Comparative visibility of planetary auroral radio emissions and implications for the search for exoplanets

Abstracts

Monday, September 26th:

Session 1 - 09:00 – 10:45 – Planetary: Jupiter

Session Chair: Philippe Zarka

[Invited] High-resolution observations of Jupiter's auroral radio emissions from Juno

M. Imai, W. S. Kurth, G. B. Hospodarsky, S. J. Bolton, and J. E. P. Connerney

Jupiter's polar auroras present complex emissions over a broad range of electromagnetic wavelengths. In the radio regime, these sources are located on auroral radio magnetic field lines. These auroral radio emissions comprise broadband kilometric (bKOM) emissions between 10 kHz and 1 MHz, hectometric (HOM) emissions between 300 kHz and 10 MHz, and decametric (DAM) emissions between a few MHz and 40 MHz. Earth-based radio observatories and near-equatorial spacecraft revealed various types of spectral structures on the timescale of milliseconds to hours. However there remains a question of whether these structures represent an intrinsic radio generation mechanism or are due to propagation effects by high density plasmas along the observer's line of sight or both. The Juno mission provides another opportunity to address this question due to its highly-eccentric, polar orbit. Juno is equipped with the Waves instrument having high resolution recording modes of electric fields from 50 Hz to 41 MHz using a dipole antenna. During each perijove pass, Juno has identified several potential radio source crossings by comparing the lower edge of the observed emission frequency with the local electron gyrofrequency based on the measured magnetic field. The emissions tend to be composed of multiple narrow band emissions, thereby forming striated spectral structures. In this presentation, we show the brief overview of Jupiter's auroral radio emissions as revealed by Juno, focusing on the high-resolution observations from its proximity to the planet and their physical implications by means of the Jovian radio beaming model.

Juno Observations of Jupiter's Synchrotron Emission and Radiation Belts

Scott Bolton, Steve Levin, Daniel Santos-Costa, Virgil Adumitroaie, Zhimeng Zhang

Juno is in a close polar orbit that passes through Jupiter's inner radiation belts providing in-situ measurements of high energy particles and dust as well remote measurements of the synchrotron emission from its unique perspective. The Juno Microwave Radiometer (MWR) measures the radio emission in 6 channels, at wavelengths ranging from approximately 1.4 to 50 cm, with 100 ms sampling throughout each spin of the spacecraft. There is a long history of Earth based observations of Jupiter's synchrotron emission using single dish radio telescopes and interferometric arrays such as the VLA. Earth based observations are constrained in viewing geometry as well as frequency due to confusion by Jupiter's atmospheric thermal emission which becomes a significant noise source at wavelengths below about 5 cm. The Juno data set provides a remarkable view of the Jovian synchrotron emission over a wide range of viewing angles, from inside the radiation belts, and provides a means of separating atmospheric thermal emission from synchrotron emission. While the MWR synchrotron data set is unprecedented, the size and variety of the data set also make analysis complex. Results from MWR will be presented along with companion data from Juno's radiation monitoring program. The Initial results comparing data against models will be presented.

Large scale numerical modeling of the jovian plasma emissions with Juno

A. Boudouma, P. Zarka, C.K. Louis, C. Briand, M. Imai

Jupiter's magnetosphere generates two kinds of radio emissions below 40 MHz: the maser-cyclotron emissions and the "plasma" emissions. The first ones are produced at high magnetic latitudes (auroral regions) by out-of-equilibrium electronic distributions, with typical energies of 1-10 keV, through a mechanism that directly converts the perpendicular energy of electrons into electromagnetic waves. The second ones, much less studied, result from the conversion of electrostatic waves at ω_L, ω_{pe}, ω_{UH} or their harmonics, into electromagnetic waves through mode conversion mechanisms. Their production involves the plasma distribution in the jovian intern magnetosphere (mainly driven by the volcanic activity of the Io satellite), and its gradients. It is these plasma emissions that we choose to study here, and to do so we propose a method from which we can derive the jovian plasma emissions macroscopic constraints based on their latitude vs. frequency diagrams obtained with the Juno/Waves observations. First, I will present the phenomenology of these emissions and their latitude vs. frequency distributions, determined from the first 3 years of Juno observations along its polar orbit [1]. Then I will describe the main theoretical frameworks for the generation of Jovian plasma emissions [2, 3] on which I based my model, as well as the models used to compute the electron density n_e [4] and the magnetic field B [5]. The modeling of the latitude vs. frequency distributions of the jovian plasma emissions is then predicted as a function of several parameters (emission frequency, angle (B, ∇n_e), $|\nabla n_e|$, direction of the emitted wave vector) for which we have systematically explored the effects. We simplify the treatment of the propagation of the radio waves between the source and the observer (straight line propagation, shadowing of the emission at ω_{pe}). Finally, the comparison between the simulated diagrams and the Juno observations is done by cross-correlation and by boolean comparisons of the latitude vs. frequency occurrence areas. I will present and interpret the results obtained in each cases and conclude on the different macroscopic constraints that we have extracted for each jovian plasma emissions.

Effect of magnetospheric disturbances on Jovian radio emissions: an in situ case study from Juno data

C. K. Louis, C. M. Jackman, A. O'Kane Hackett, E. Devon-Hurley, W. S. Kurth, G. Hospodarsky, P. Louarn, F. Allegrini, J. E. P. Connerney, D. M. Weigt, S. McEntee, A. R. Fogg, J. E. Waters, S. J. Bolton

During its 53-day polar orbit around Jupiter, Juno often crosses the boundaries of the Jovian magnetosphere (namely the magnetopause and bow shock), as well as the plasma disc (located at the centrifugal equator). The positions of the magnetopause and bow shock allow us to determine the dynamic pressure of the solar wind (using both the updated model of Joy et al. 2002 by Ranquist et al., 2020 and/or in situ data) which allows us to infer magnetospheric compression or relaxation, while the observations of plasma disc perturbations allow us to infer magnetospheric reconfigurations. The aim of this study is to examine Jovian radio emissions during magnetospheric disturbances, in order to determine the relationship between the solar wind and Jovian radio emissions. In this presentation, we show case studies for each typical case (bow shock, magnetopause and plasma disk crossing). We show that the activation of new radio sources is related to magnetospheric disturbances. The perspectives are to carry out a statistical study of these crossings. We hope to be able to show a relation between the activation of new radio sources (intensity and extension of the emission, position of the sources) and the solar wind (dynamic pressure, magnetic intensity, ...). The final objective is to be able to use observations of the planetary radio emission as a proxy for the solar wind.

Ground support of Juno mission and data preprocessing

Vyacheslav Zakharenko; Viktoriia Kharlanova; Vladimir Ryabov; Serge Yerin; Brazhenko Anatoly; Anatoly Fransuzenko; Oleksandr Konovalenko

Since 2016, the spacecraft Juno has been operating in the orbit of Jupiter. The Juno spacecraft program was originally designed for 36 revolutions around Jupiter with a period of about 53.5 Earth days. In June 2021, the mission was extended until 2025, or until the device fails. Ukrainian low-frequency radio telescopes [1] (primarily UTR-2) conduct constant observations together with the Juno spacecraft as part of ground support missions. Each year, 7 observation sessions are held, which last 2-4 days. As a rule, perijove (PJ) do not coincide with the maxima of the storms of S-bursts, controlled by satellites Io and Ganymede. However, the sensitivity of UTR-2 allows the detection of low-intensity radiation of various types of bursts. The observations at the UTR-2 radio telescope are carried out in two modes: - correlation mode of signals of North-South and East-West antennas of UTR-2 with two receivers [2]: beam ON – direction to Jupiter, beam OFF – 1° away from Jupiter, - waveform mode (WF): only one receiver, beam ON. In addition, starting from June 2019, observations of radio emission from Jupiter, which are controlled by the satellites Io and Ganymede, are being carried out. These studies are conducted in conjunction with the newly built NenuFAR telescope (Nancay, France). Also, observations are carried out on the URAN-2 radio telescope with the possibility of polarization studies. Observation data from the UTR-2, URAN and GURT telescopes are stored on a server in Japan (Future University, Hakodate). The data of the Juno mission's ground support radio telescopes will be compared with the data of the spacecraft in order to search for new features or types of radio emission from Jupiter. The biggest problem that an observer in the low-frequency range faces is radio frequency interference (RFI). The varying drift velocity of S-bursts, the random time of occurrence, and the absence of a simple law of frequency variation with time (in contrast to a linear frequency dependence or a quadratic one, characteristic, for example, for the dispersion delay of pulsed radio emission from pulsars) do not allow one to single out S-bursts by a certain frequency-time "window". The task is to improve the RFI mitigation utilities. It is necessary to use both the available information about the nature of RFI, and to use new approaches for their recognition. This will allow analyzing with greater accuracy the characteristics of different radio bursts, as well as facilitating the physical interpretation of the mechanisms that generate radiation.

Session 2 - 11:15 – 12:30 – Planetary: Jupiter

Session Chair: Corentin Louis

Electron densities in Jupiter's polar regions: Implications for the generation of auroral and radio emissions

A. H. Sulaiman, W. S. Kurth, S. S. Elliott, G. B. Hospodarsky, O. Santolík, L. Lamy

A major objective of the Juno mission to explore Jupiter's high-latitude magnetosphere and ionosphere. The Waves instrument has provided information from which electron densities may be inferred. Near Juno's perijove passes the cyclotron frequency (fce) often exceeds the plasma frequency (fpe) by three orders of magnitude, representing space plasma conditions not previously met in planetary missions. Techniques to infer electron densities are applied by extending theoretical treatments of plasma waves into highly magnetized regimes. Here we present electron densities in Jupiter's polar regions and reveal well-defined depletions on magnetic flux tubes that connect to the main auroral emissions. We discuss the important implications of density constraints on: (i) the development of parallel potential structures capable of accelerating auroral electrons and driving ion outflow, (ii) the dissipation of Alfvén waves that are capable of accelerating auroral electrons, and (iii) the generation of radio emissions, which requires a low fpe/fce.

Characterization of jovian decametric auroral emissions (DAM) using in situ radio and electron data

Brieuc Collet, Laurent Lamy, Corentin Louis, Philippe Zarka, Renée Prangé, Ali Sulaiman, W. Kurth

The Juno spacecraft is orbiting around Jupiter since mid-2016 and has crossed regularly the auroral radio emission regions of both hemispheres, ranging kilometric to decametric radiosources, during which electrons and auroral radio waves were sensed in situ. Over the 10 first perijoves, we first obtain evidences of a systematic spatial conjugacy between the crossed radiosources and the zone of diffuse aurora. Applying the measured electron distribution functions (using JADE-E and MAG experiments) to the theoretical expressions from the electron maser cyclotron instability theory, we then computed both the expected growthrate and the wave intensity, which we compared to the wave flux density as derived from Juno/Waves calibrated observations. On top of the 2 CMI sources of free energy previously identified (loss cone electron distribution function and conics), we show that shell-type electron distribution functions reminiscent of the terrestrial and kronian cases can also drive powerful radio emissions.

Determining the beaming of Io decametric emissions : a remote diagnostic to probe the Io-Jupiter interaction

L. Lamy, L. Colomban, P. Zarka, R. Prangé, M. S. Marques, C. Louis, W. Kurth, B. Cecconi, J. Girard, J.-M. Griessmeier, S. Yerin

We investigate the beaming of 11 Io-Jupiter decametric (Io-DAM) emissions observed by Juno/Waves, the Nançay Decameter Array and NenuFAR. Using an up-to-date magnetic field model and three methods to position the active Io Flux Tube (IFT), we accurately locate the radiosources and determine their emission angle θ from the local magnetic field vector. These methods use (i) updated models of the IFT equatorial lead angle, (ii) ultraviolet (UV) images of Jupiter's aurorae and (iii) multi-point radio measurements. The kinetic energy E(e-) of source electrons is then inferred from theta in the framework of the Cyclotron Maser Instability. The precise position of the active IFT achieved from methods (ii,iii) can be used to test the effective torus plasma density. Simultaneous radio/UV observations reveal that multiple Io-DAM arcs are associated with multiple UV spots and provide the first direct evidence of an Io-DAM arc associated with a trans-hemispheric beam UV spot. Multi-point radio observations probe the Io-DAM sources at various altitudes, times and hemispheres. Overall, theta varies a function of frequency (altitude), by decreasing from 75-80° to 70-75°over 10-40 MHz with slightly larger values in the northern hemisphere, and independently varies as a function of time (or longitude of Io). Its uncertainty of a few degrees is dominated by the error on the longitude of the active IFT. The inferred values of E(e-) also vary as a function of altitude and time. For the 11 investigated cases, they range from 3 to 16 keV, with a 6.6 +/- 2.7 keV average.

Statistical Study on the Jovian Decametric Radio Emissions Based on Multiple-view Observations from Remote Radio Instruments [online]

Ruobing Zheng, Yuming Wang, Xiaolei Li, Chuanbing Wang, and Xianzhe Jia

To better understand the physical processes associated with Jovian decametric (DAM) radio emissions, we present a statistical study of DAMs and inferred characteristics of DAM sources based on multi-view observations from the Wind and STEREO spacecraft. Altogether 111 isolated strong events in radio dynamic spectra are analyzed from 2008 to 2014. The apparent rotation speed of DAMs derived from multiple spacecraft can be used to distinguish Io-related and non-Io-related DAMs. We find that the rotation speed of Io-related DAMs is in the range of 0.15–0.6 Ω_J and that of non-Io-DAMs is between 0.7–1.2 Ω_J, and the Io-DAMs are approximately 6.3 times more likely to occur than non-Io-DAMs. We locate the sources of the 68 DAMs (including 10 events observed by the Nançay Decameter Array) and infer their emission angles and associated electron energies. The statistical results show that the DAM source locations have three preferred high-latitude regions, two in the southern hemisphere (around 50° to 140° and around 250° to 360° in System III longitudes) and one in the northern hemisphere (around 160° to 200°), which is probably caused by the non-symmetrical topology of Jupiter's magnetic field. The difference between Io-DAM source footprints and Io auroral spots changes with Io’s position in System III longitude, consistent with the previous results from Hess et al. (2010), Bonfond et al. (2017) and Hinton et al. (2019). In addition, the emission angles for non-Io-DAMs are smaller than those for Io-DAMs from the same source regions and all the emission angles range from 60° to 85°. Correspondingly, the energies associated with the electrons responsible for exciting the radio emissions are estimated to range between 0.5 and 20 keV.

Session 3 - 14:00 – 15:30 – Planetary: Lightning + Auroral Kilometric Radiation

Session Chair: Joe Kinrade

New insights into Jovian lightning thanks to high-resolution electromagnetic measurements onboard Juno

Ivana Kolmasova, Ondrej Santoli, Masafumi Imai, William S. Kurth, George B. Hospodarsky, Scott. J. Bolton, and John E. P. Connerney

Past investigations of time scales of lightning processes on Jupiter were substantially limited by characteristics of instruments onboard Voyager, Cassini, Galileo and New Horizons missions. Due to long camera exposure times (6 s – 3 min) optical lightning detections probably contained overlaid lightning strokes. The radio receiver onboard Voyager 1 recorded individual lightning whistler traces with an average rate reaching 1 whistler per second.

Thanks to the unique orbit of the Juno spacecraft two new types of electromagnetic signals induced by Jovian lightning were discovered in the measurements of the Waves instrument: extremely low dispersion whistlers and discrete dispersed pulses. Both types of lightning induced signals were routinely observed by the Waves receiver during all scientific perijove passes of the prime Juno mission. Low dispersion rapid whistlers were recorded at frequencies from 50 Hz to 20 kHz, and the Jovian dispersed pulses (JDPs) were collected at frequencies between 10 kHz and 150 kHz.

A high sampling frequency of the Waves receiver allows us to distinguish individual whistler traces even if they are separated by as little as 3 milliseconds. Individual JDPs can be distinguished if they are separated by only about 250 microseconds. The accumulated dispersion of the individual rapid whistlers is very low varying from several milliseconds to a few tens of milliseconds. The dispersion of JDPs is even lower. Such a low dispersion indicates the presence of regions with very low ionospheric density.

In this study, we present the latitudinal, longitudinal and altitudinal variations in the occurrence rates of lightning whistlers with different frequency drift rates . We also characterize the time scales of lightning processes on Jupiter by investigating the time separations of JDPs or whistler traces within individual waveform snapshots. We compare obtained results with properties of terrestrial lightning.

Propagation of radio waves from lightning discharges through the Jovian ionosphere

Ondrej Santolik, Ivana Kolmasova, Masafumi Imai, George B. Hospodarsky, William S. Kurth, Scott. J. Bolton, and John E. P. Connerney

Lightning discharges on Jupiter have been discovered using measurements of the Voyager 1 spacecraft in 1979. Radio waves generated by lightning have been first observed in the dense plasma of Io torus where the original short impulsive signals from Jovian atmosphere were dispersed by their passage through the plasma medium. They were discovered by Gurnett et al. (1979) in the form of whistlers at time scales of several seconds and at frequencies of several kHz.

The unique polar orbit of the Juno spacecraft allows us to observe radio waves generated by lightning in the topside ionosphere very close to Jupiter. As their path through the plasma is short, the accumulated dispersion is low, and the time scales of these rapid whistlers decrease to several tens of milliseconds, but sometimes impulsive signals with negligible dispersion are observed at times scales of milliseconds.

We use two-component electromagnetic measurements of the Juno Waves instrument to observe previously unknown effects of radio wave propagation from lightning discharges through the low-density plasma in the ionosphere of Jupiter. A large local magnetic field modifies the dispersion relation, leading to unusual frequency dependent group delays, which are not observed in the relatively dense ionosphere of the Earth.

Jupiter Long Dispersion Lightning Whistlers associated with the Io torus: Juno Observations

G. B. Hospodarsky, W. S. Kurth, M. Imai, I. Kolmašová, O. Santolík, J. E. P. Connerney, and S. J. Bolton

The detection of lightning whistlers by the Voyager spacecraft provided the first conclusive proof of atmospheric lightning on Jupiter. Voyager detected these lightning whistlers in different regions of the Io torus, between ~5 and 6 Jovian radii. The whistlers exhibited dispersive curves with time scales of a few seconds, and the shape and time scale of this dispersion provided estimates of the density profile along the whistler propagation path. The Juno spacecraft, with its multiple polar orbits is providing a new opportunity to examine the properties of lightning whistlers at Jupiter and investigate the density characteristics of the plasma they propagate through. During most perijove passes, the Waves instrument on Juno detects shorter dispersion lightning emissions. Below 20 kHz, both electron and ion whistlers are detected with dispersive curves with time scales of a few to 10s of mS. At higher frequencies (~20 to 150 kHz), a lightning related emission consisting of dispersed millisecond pulses named Jupiter dispersed pulses (JDPs) is often detected. These emissions have dispersion curves much shorter than the Voyager observations, suggesting a much shorter propagation path from the lightning source and the spacecraft, which has been verified from wave propagation direction analysis. As the Juno mission has progressed, the Juno orbit has changed such that the spacecraft is often on magnetic field lines that pass through the Io torus at lower latitudes. During many of these periods, longer dispersion (many seconds) lightning whistlers have been detected, very similar to those detected by Voyager. We will discuss the conditions under which that these emissions are detected, the properties of the emissions, and examine the density profile of the Io torus needed to produce the observed spectral characteristics of these longer dispersion whistlers.

Advances in leaked Auroral Kilometric Radiation

James LaBelle, Keith Yearby, and Jolene Pickett

Accumulating evidence suggests that Auroral Kilometric Radiation (AKR) propagates downward in the whistler mode in addition to the well-known escaping AKR beamed outward which is primarily X-mode. The downward propagating component is known as "leaked" AKR [Oya et al., 1985]. Antarctica is the ideal location for detecting leaked AKR due to absence of man-made interference. Leaked AKR has been measured at South Pole for four consecutive years, 2018-2021. AKR is distinguished from auroral hiss, which occurs in the same frequency band, by its fine structure which is similar to that of escaping X-mode AKR observed in space. Presumably because of required propagation conditions, AKR reaches ground level only during the depths of winter at South Pole, late May to late August, when the overhead ionosphere is not illuminated by the sun. The frequency distribution of ground-level leaked AKR overlaps with the high-frequency end of the distribution of escaping AKR, implying sources at relatively low altitudes. The polarization is right-handed as expected for whistler mode. As with the escaping X-mode AKR sources, ground-level leaked AKR is most prevalent in the midnight magnetic local time sector. Bursts of ground-level AKR have been observed correlated with similar bursts of escaping AKR measured with the Geotail and Cluster satellites. On rare occasions, similar fine structure occurs in AKR observed at South Pole and simultaneously with the Cluster satellites. The narrowband nature of the leaked AKR, as well as its occasional correlation with simultaneous escaping AKR, argues against generation over a range of altitudes well below the acceleration region, for which broadband radiation is expected. Instead, it seems likely that leaked AKR is generated in the direct vicinity of the escaping AKR sources, possibly through mode conversion of Z-mode waves which are excited by the cyclotron maser instability in the same and nearby locations where that instability produces escaping X-mode waves. The consistent observations of leaked AKR at ground level in Antarctica motivates renewed effort to explain this phenomenon and presents opportunities to remotely sense the auroral acceleration region from the ground as has been done from space using escaping AKR.

Classification of the spectral fine structure in Auroral Kilometric Radiation

Ulrich Taubenschuss, Georg Fischer, David Pisa, Ondrej Santolik, and Jan Soucek

Auroral kilometric radiation (AKR) is known to be generated by unstable electron populations in the auroral region of Earth's magnetosphere. Weak background radiation becomes amplified by the cyclotron maser instability through interaction with hot electrons exhibiting a horseshoe or shell distribution in velocity space. However, the shell maser mechanism alone can not explain frequent observations of AKR spectral fine structure when recorded with sufficiently high time and frequency resolution, like the so-called striations or very narrowbanded emission drifting rapidly up and down in frequency. We will present observations from the Cluster Wideband Receiver (WBD) dataset and provide an overview of the different types of AKR spectral fine structures. The WBD can be connected to one of two electric double-probe antennas onboard Cluster, and it is sampling electric waveforms with sampling rates up to 220 kHz. These data also frequently contain signals from AKR. A classification scheme and relevant statistics for the different types of AKR fine structure will be presented. Possible source mechanisms for fine structures like transient electron holes and ion holes as elementary radiators will be discussed.

Novel Wind/Waves AKR Observations and Use in Exploring Magnetospheric Dynamics

J. E. Waters, C. M. Jackman, D. K. Whiter, L. Lamy, A. R. Fogg, B. Cecconi, X. Bonnin, K. Issautier, C. Forsyth

Terrestrial Auroral Kilometric Radiation has been extensively studied and its fundamental properties are well-known. Long term observations have often been discounted, however, due to the non-trivial isolation of radio emission of a particular source and a lack of instrumentation covering the necessary timescale. We have developed a novel selection of AKR that can be applied to Wind/Waves to unlock decades of observations from a wide variety of viewing positions. Using the time variability of AKR and the spin period of Wind/Waves, solar radio and background emissions are effectively removed from the data and AKR observations are fully calibrated. With studies on both statistical and case study bases, we explore the dynamics of different magnetospheric regions. Remote AKR observations with Wind exhibit dependencies on the spacecraft latitude and local time that depict radio source beaming properties and their longitudinal distribution. We compare the average AKR power in higher and lower frequency bands with event lists of substorms, derived by

observations of various magnetospheric phenomena. In this way, for the first time, we begin to quantify the discrepancy in the dynamics of the upper and lower auroral acceleration region across differing event sizes. Further AKR observations from L1, exhibiting dayside acceleration processes, follow the impact of an interplanetary coronal mass ejection and are presented with other geomagnetic indices; these results show the promise of future explorations of these observations. Future analyses will explore unprecedented timescales and viewing positions, with a rich dataset that covers multiple solar cycles.

Session 4 - 16:00 – 17:30 – Posters session

Session Chair: Caitriona Jackman

See the list of poster abstracts.

Tuesday, September 27th

Session 5 - 09:00 – 10:45 – Solar

Session Chair: Diana Morosan

[Invited] Insights on solar-stellar atmospheric activity from modern sensitive radio and mm-arrays [online]

Mohan, Atul

Millimeter to radio waveband collectively probe the activity across the hot outer atmospheric layers of the sun and cool stars. While metrewavebands are sensitive to emission from various coronal layers, millimeter band is sensitive to thermal emission from layers across chromosphere to corona. Previous decade witnessed the dawn of sensitive interferometric arrays across mm - radio band, facilitating snaphot spectroscopic imaging studies at spectro-temporal cadence like never before. My talk will broadly cover the novel insights gained using data from modern metrewave arrays like MWA, LOFAR etc and the mm array, ALMA. In the case of the Sun, modern metrewave instruments have helped produce spatialy resolved dynamic spectra for the quiet and active solar corona at sub-second and sub-MHz resolution. Studies of radio bursts using such spatially resolved spectra have lead to discoveries of novel modes of quasi-periodic pulsations and spectro-temporal fine strutures. Tracking the fine spectro-temporal structural evolution of coronal radio sources, have revealed crucial features of coronal turnbulence and density inhomogenieties. Meanwhile in mm band ALMA opened a window into high cadence solar/stellar chromospheres. Due to its supreme sensitivity and high angular resolution (~ few to sub arcsec) in this band, it is now possible to do sensitive high resolution studies of solar chromoshpere. Besides, the high sensitivity lets us explore the chromospheric structure and activity in cool stars within ~ 10 - 20 pc, lettting us define novel robust indicators of solar/stellar activity which let us explore the links between atmospheric structure, stellar physical paramters and emergent activity.

The frequency ratio and time delay for solar radio emissions with fundamental and harmonic components

Xingyao Chen, Eduard P. Kontar, Daniel L. Clarkson, Nicolina Chrysaphi

Solar radio bursts generated through plasma emission processes may produce radio fundamental emission at the local plasma frequency (F) and its second harmonic (H). There is one long-standing problem that the theory of plasma emission gives a harmonic frequency ratio to be close to 2, yet observations show an average of 1.8. We present LOFAR observations of F and H components of three type III bursts with striae fine structures. The harmonic frequency ratios are between 1.62 and 1.75 between 30-39 MHz. We explain this by considering that the F and H components emit at the same location, but the onset of F emission is delayed with respect to the H emission. We state that the observed delay time can not be explained by different group velocities of the F and H emissions; instead, the interpretation of radio-wave propagation with anisotropic radio-wave scattering in turbulent corona is required. Combined with ray-tracing simulations, for the first time, we quantitatively predict the relations between the frequency ratio and delay time due to radio wave propagations effects. The time delay should be considered for the spectral imaging analysis of F and H emissions.

Radio-wave Scattering Effects on Observations of Solar Radio Spikes and Type IIIb Striae Within a Closed Loop System

Daniel L. Clarkson, Eduard P. Kontar, Nicole Vilmer, Mykola Gordovskyy, Xingyao Chen

We present a statistical analysis of spatially, frequency, and time resolved individual solar radio spikes within a trans-equatorial coronal loop using the LOw Frequency ARray (LOFAR), and compare with fine frequency structures of type III emission (striae). Spikes and striae in close temporal proximity at the same frequency are observed to have co-spatial radio contours near 45 MHz, with increased separation towards 30 MHz. Fixed frequency imaging of both spikes and striae between 30-45 MHz reveals centroid motion parallel to the solar limb, with comparable, and frequency dependent trajectories. The plane-of-sky spike centroid velocities are often superluminal, independent of frequency in the observed range, and consistent with radio-wave scattering simulations with strong anisotropy of the density fluctuation spectrum. Spike and striae bandwidth distributions share the same peak and spread, indicating the emission of each burst type passes through density inhomogeneities with comparative spatial scales. Comparison of decameter spike characteristics with those in the hundreds of megahertz to gigahertz range shows a discontinuity in spike bandwidths near 200 MHz, suggesting that the higher frequency observations are spectrally limited in resolution. The observed emission properties of each burst type are consistent with the interpretation of radio-wave scattering in an anisotropic turbulent medium. The spike decay time and source sizes across all considered frequencies follows a consistent trend, suggesting that scattering effects are significant in both frequency domains.

Meter-decameter observations of "fractured" type II solar radio bursts

Artem Koval, Marian Karlický, Aleksander Stanislavsky, Bing Wang, Serge Yerin, Aleksander Konovalenko, Miroslav Bárta

In this work, we report about meter-decameter radio observations of solar type II bursts demonstrating fractured spectral shapes on solar dynamic spectra. These bursts are attributed to collisions of shock waves with different coronal density structures. Two case studies with "fractured" type II bursts have been examined. In the first one, two successive type II bursts having spectral break and spectral bump were used as probes to obtain magnetic field variations in coronal structures, namely a coronal streamer and flux tube. In the second case study, type II burst showing herringbone pattern and spectral break was analyzed to study turbulent plasma density irregularities inside a coronal streamer. In both cases, the most feasible scenarios of the CME-streamer interactions and positions of radio-emitting sources within the shock waves have been considered. The results have direct impact on interpretations of spectrally fractured type II bursts and contribute to the current studies on the solar wind sources to which streamers and flux tubes belong.

On the source sizes of fine structures of type II radio bursts using LOFAR

Anshu Kumari, Diana E. Morosan, Emilia K. J. Kilpua, Leopekka Sarasta, Pietro Zucca

The magnetic field dominates the structure and dynamics of the solar corona and it is the primary driver of Space weather. Radio observations are one of the most common approaches to diagnosing the magnetic field in the solar atmosphere. One of the direct signatures of explosive solar phenomena, such as coronal mass ejections (CMEs) in radio wavelengths, is called metric type II radio bursts. Type II bursts originate from plasma waves converted into radio waves at the local plasma frequency and its harmonics. These radio bursts can be considered a direct diagnosis of MHD shocks in the solar atmosphere. These bursts can be used to study the kinematics, energetics, and dynamics of the associated eruptive events. With state-of-the-art radio instruments such as LOw Frequency ARray (LOFAR), it has now been possible to study these bursts and the structures within them in great spectral, temporal and spatial resolutions. We studied the source sizes and shapes of the fine structures of type II radio bursts observed with LOFAR and their variation with frequency in metric wavelengths.

Double plasma resonance model of solar radio zebras

Jan Benáček and Marian Karlický

Solar radio fine structures of Type IV bursts are an excellent tool for plasma diagnostics during solar flares. One of their models is the electron cyclotron maser instability based on the double plasma resonance between electron cyclotron and plasma frequencies and an unstable wave in the presence of a loss-cone type of the velocity distribution. The radio emission occurs in the electromagnetic Z-mode along the magnetic field or at the harmonic of the X-mode in the perpendicular direction. However, it is unclear where and how the instability evolves and how the locally captured electrostatic waves are converted to escaping radio waves. To obtain the instability evolution, we calculated its growth rates and saturation energies as functions of cyclotron-to-plasma frequency ratio and plasma parameters by using analytical calculations and particle-in-cell simulations. We found that the growth rates and saturation energies are maximal, approximately at the integer harmonics of the cyclotron frequency. The maxima shift to lower frequencies with increasing the plasma temperature; they broaden and decrease with increasing the harmonic number. We also found that large loss-cone angles are necessary to explain the detected high harmonic numbers of zebras, which may exceed one hundred. Moreover, we estimated electromagnetic energy densities in the emission region and the conversion efficiency to the radio waves.

Session 6 - 11:15 – 12:45 – Solar ground-based

Session Chair: Pietro Zucca

First detailed polarimetric study of a group of type III solar radio bursts with the Murchison Widefield Array [online]

Soham Dey, Devojyoti Kansabanik, Divya Oberoi

Type III solar radio bursts result from streams of energetic electrons travelling outwards along the open magnetic field lines through the hot magnetised coronal plasma. Hence their study can enable us to have a better understanding of the coronal plasma and its effect on the propagation of electromagnetic waves through it. Their polarimetric studies are mostly limited to the analysis of their dynamic spectra, which do not provide any spatial information. But now with the emergence of new generation radio telescopes, like the Murchison Widefield Array, and our robust full Stokes calibration and imaging pipeline, referred to as P-AIRCARS (Kansabanik et al., 2022), we are now able to produce high fidelity and high dynamic range spectro-polarimetric snapshot low-frequency solar images. This allows us to explore the polarimetric properties of these bursts in hitherto inaccessible details. This has led to some interesting discoveries. Theoretically, one expects highly circularly polarised emission from type-III bursts and any traces of linear polarisation, if present, are expected to be washed out due to the differential Faraday rotation in the corona. We have for the first time found convincing image-based evidence of linear polarisation from type-III radio solar bursts at metre wavelengths. Surprisingly, the linear polarisation fraction is larger than the circular polarisation fraction and also shows anti-correlation with the circular polarisation. This indicates towards the conversion of circularly polarised emission to linear polarisation as the electromagnetic waves propagate through the magnetised corona. Here we present the current status of our investigation of these type-III radio bursts.

Coronal Magnetic Field Measurement during Quiet Time using Low-Frequency Spectropolarimetric Imaging [online]

Devojyoti Kansabanik, Surajit Mondal, Divya Oberoi

The so-called “quiet corona” is not so quiet at all. The electron density, temperature, and magnetic field strengths are lower in the quiet Sun regions, as compared to the active regions, but there are still dynamic. As the quiet corona provides the background environment in which all of the coronal dynamics and eruptive phenomena take place, it is important to estimate the plasma parameters of the ambient quiet corona. At higher coronal heights (more than 1.3 solar radii), the emissivity of the corona becomes too low to be measurable in visible, EUV, and X-ray bands. It is hence hard to measure the physical parameters of the corona at higher coronal heights using these observing bands. Low-frequency radio observations are particularly suitable for gathering this information. Using new-generation radio interferometers, like the Murchison Widefield Array (MWA), it is now possible to make high dynamic range spectro-polarimetric solar images of the Sun. Our recently developed robust polarization calibration and imaging pipeline deliver imaging dynamic ranges spanning a few hundred to 105 with very low residual instrumental polarization (less than 0.05%). These images can provide the means to estimate the coronal electron density and temperatures at higher coronal heights routinely. Also, though thermal emission is unpolarized, on passing through the inhomogeneous magnetized coronal plasma it picks up a weak circular polarization (less than 1%) due to the birefringent nature of this medium. It is possible, in principle, to measure the large-scale quiet Sun coronal magnetic field by measuring this weak circular polarization. We present the first-ever detection of circular polarization from quiet Sun thermal emission and use it to estimate the large-scale ambient coronal magnetic field. This forms a convincing demonstration that high fidelity spectro-polarimetric imaging at low radio frequencies provides a novel method for 26 estimating the physical parameters of the corona.

Observations and Modeling of The Quiet Solar Corona in Low Frequency Imaging
Kamen Kozarev, Peijin Zhang, Pietro Zucca, Eoin Carley

The radio emission of the quiet Sun in the metric and decametric bands has not been well studied historically due to limitations of existing instruments. It is nominally dominated by thermal bremsstrahlung of the solar corona, but may also include significant gyrosynchrotron emission, usually assumed to be weak under quiet conditions. In this work, we investigate thermal and gyrosynchrotron solar radio emissions in the lowest radio frequencies observable by ground instruments, for different regions of the low and middle corona. Observations were made with We approximate the coronal conditions by a synoptic magnetohydrodynamic (MHD) model. The thermal emission is estimated from a forward model based on the simulated corona. Additionally, we calculate expected gyrosynchrotron emission. The model results are compared with quiet-time interferometric imaging observations between 20-250 MHz by the LOw Frequency ARray (LOFAR) radio telescope. The contribution of gyrosynchrotron radiation to low frequency solar radio emission may shed light on effects such as the hitherto unexplained brightness variation observed in decametric coronal hole emission, and help constrain measurements of the coronal magnetic fields.

Automatic detection of radio bursts in NenuFAR solar observations
Pearse C. Murphy, Stéphane Aicardi, Carine Briand, Eoin P. Carley, Baptiste Cecconi

Solar radio bursts are some of the brightest emissions at radio frequencies in the solar system. The emission mechanisms that generate these bursts offer a remote insight into physical processes in solar coronal plasma, while fine spectral features hint at its underlying turbulent nature. During radio noise storms many hundreds of solar radio bursts can occur over the course of a few hours. Identifying and classifying solar radio bursts is often done manually although a number of automatic algorithms have been produced for this purpose. The use of machine learning algorithms for image segmentation and classification is well established and has shown promising results in the case of identifying Type II and Type III solar radio bursts. Here we present the results of a convolutional neural network applied to dynamic spectra of NenuFAR solar observations. We highlight some initial success in segmenting radio bursts from the background spectra and outline the steps necessary for burst classification.

The escape and propagation of shock-accelerated electron beams during a solar coronal mass ejection
Diana E. Morosan, Jens Pomoell, Anshu Kumari, Rami Vainio and Emilia K. J. Kilpua

Energetic particle populations are ubiquitous throughout the Universe and often found to be accelerated by astrophysical shocks. One of the most prominent sources for energetic particles in our solar system are huge eruptions of magnetised plasma from the Sun called coronal mass ejections (CMEs), which usually drive shocks that accelerate charged particles up to relativistic energies. Accelerated electrons, in particular, can be observed either remotely as low-frequency radio bursts or in situ as large particle fluxes detected by spacecraft. However, it is currently unknown where electrons accelerated in the early phases of such eruptions propagate and when they escape the solar atmosphere. Here, we report the first results on the acceleration, escape, and propagation directions of electrons during the early evolution of a strongly expanding and high Mach-number CME-driven shock. The study uses a three-dimensional (3D) representation of the particle acceleration locations in relation to the overlying coronal magnetic field, CME propagation, magneto-hydrodynamic (MHD) models of the solar corona, and radio spectropolarimetric and imaging observations from ground-based observatories. The synthesis of these methods allow us to combine in a unique manner the temporal evolution of the location of radio sources to the location of the expanding low coronal CME shock. We show convincing evidence that the first radio emission in the CME eruption comes from electrons that initially propagate in regions of low Alfvén speeds and along closed magnetic field lines. This is in contrast with electrons that in later stages escape along open field lines.

Session 7 - 14:00 – 15:30 – Solar space-based

Session Chair: Peter Gallagher

[Invited] Low-frequency solar radio astronomy in the era of Parker Solar Probe and Solar Orbiter

Stuart D. Bale, Milan Maksimovic, Vratislav Krupar, and Marc Pulupa

Interplanetary (IP) low-frequency (LF) radio emission is a primary remote-sensing signature of suprathermal electrons associated with flares, CME-driven shock, CIRs, and planetary foreshocks. While the general scenario of IP radio emission is mostly understood, new measurements from the Parker Solar Probe/FIELDS instrument and the Solar Orbiter/Radio and Plasma Waves (RPW) suite are revealing new phenomena. In particular, higher spectral resolution measurements reveal fine structure that is likely to be associated with plasma density inhomogeneities. New measurements of the magnetic component of both o-mode radio and z-mode waves are pointing more directly towards particular radio emission mechanisms. And of course, multi-point measurements using PSP, SO, STEREO, and Wind now allow refined time-of-arrival analysis of large-scale magnetic field structure as type III bursts move along the IP magnetic field. I will review some of these new observations and provide some perspective on what's ahead.

Simultaneous Observations of Solar Radio Bursts using LOFAR and Spacecraft Instruments

Mohamed Nedal, Kamen Kozarev, Pietro Zucca, Peijin Zhang

Solar radio bursts are often associated with eruptive phenomena during which the electrons are accelerated and energy is exchanged in the solar corona. Type-III radio bursts are usually generated by electron beams traveling along open magnetic field lines. In addition, multi-viewpoint observations of solar radio bursts observed by widely separated remote instruments allow probing fundamental characteristics of the corona's emission mechanisms and plasma conditions.

In this work, we combine the dynamic spectra observed by instruments on the Parker Solar Probe (PSP), Solar Terrestrial Relations Observatory (STEREO), and Wind spacecraft, with observations by the Low-Frequency Array (LOFAR), extending the frequency range to 2.6 kHz – 190 MHz. Then we perform spectral analysis on the combined spectra of type-III radio bursts, extract information relevant to the source of emissions in the lower corona, and compare the characteristics of bursts between in-situ and remote observations. We also investigate the influence of the relative positions of the instruments on the measurements since the radio bursts may be modified by reflection and/or scattering as the emission propagates through the corona.

Type III Bursts and Solar Energetic Particles

Krupar, V. ; Szabo, A. ; Kruparova, O. ; Richardson, I. G. ; Martinez Oliveros, J. C. ; Narock, A. ; Pasanen, J.

Type III bursts are manifestations of energetic electrons associated with solar flares. Since propagation of radio waves in the interplanetary medium is strongly affected by random electron density fluctuations, interplanetary type III bursts provide us with a unique diagnostic tool for solar wind remote plasma measurements. We developed a type III burst automated recognition tool applicable to the Wind and STEREO measurements in order to build an extensive database of radio events. We compared parameters of radio bursts associated with solar energetic particles (SEPs). We investigate possible correlations between solar flares, type III bursts, and SEP events. We discuss possible capabilities of real-time interplanetary radio observations, including direction-finding, to enhance current SEP forecasting.

Low Frequency Radio Emission Associated with an Impulsive Flare and Coronal Mass Ejection

Jeremy Rigney, Peter T. Gallagher, Eoin P. Carley, Gavin Ramsey, Gerry Doyle, Laura Hayes, Pietro Zucca

An impulsive X1.5 solar flare, coronal mass ejection, EUV wave and numerous radio bursts occurred on 2022 May 10 from active region NOAA AR3006. The Irish Low Frequency ARray (I-LOFAR) was observing the Sun with the REALtime Transient Acquisition (REALTA) backend at the time, providing 1 millisecond dynamic spectra at 10-240 MHz. Many type IIIs and a type II were detected with I-LOFAR/REALTA. In addition, radio images at 150 MHz were obtained from the Nançay Radio Heliograph. The 150 MHz radio sources were contemporaneous with the type II and located in close proximity to the leading edge of the associated coronal mass ejection. In this talk, we examine the radio emission from this event, focusing on the location and movement of the source of radio emission detected by NRH and fine structure in the type II radio burst. These observations give an insight into the excitation of a shock wave associated with the EUV wave and CME and the acceleration of energetic electrons.

Offset Measure: Quasars as detector for electron density in solar atmosphere and inner heliosphere

Peijin Zhang, Kamen Kozerev, Pietro Zucca, Eoin Carley

Solar atmosphere electron density is an important parameter in the space weather study. In this work, we present the observation of position offset of radio sources near the Sun, the value of offset value is frequency dependent. From the relation of the frequency and offset distance, we can derive an offset measure (OM) representing the total refraction effected on the line of sight(LOS) of the radio source. This work shows the possibility of mapping the electron density of the Solar atmosphere.

Session 8 - 16:00 – 18:00 – Space Weather & Posters

Session Chair: Pearse Murphy

[Invited] Radio techniques for Space Weather [online]

Klein, Ludwig

Radio astronomical observations offer relatively simple and cheap possibilities to monitor solar and interplanetary phenomena that may have impact on the space environment of the Earth. In this talk I will attempt to give an overview of features that are or can be used in space weather services: (1) Flux density measurements of the quiet Sun at microwave frequencies are a demonstrated proxy of EUV intensity that can be used to monitor the heating of the Earth's atmosphere and its influence on spacecraft in low-Earth orbit. (2) Flux densities of radio bursts show some correlation with the speed of coronal mass ejections (CMEs), which can be exploited to estimate travel times from Sun to Earth. (3) The occurrence of major CMEs themselves is revealed by characteristic metre-wave emission, called type IV bursts, before the features emerge from behind the occulting disk of white-light coronagraphs. (4) There are also a variety of applications to solar energetic particles, ranging from the question whether energetic particles escape from the solar corona to the interplanetary space to the magnetic connection between the Sun and a spacecraft. (5) On occasion, solar radio emissions can be a space weather hazard of their own, perturbing the functioning of cell phones and air traffic control radar.

Incremental Development of LOFAR Space-Weather – IDOLS

P. Zucca, K. Kozarev, P. Zhang, M. Nedal, M. Mevius, E. Carley, S. Maloney, M. Mancini, R. Miteva

IDOLS stands for Incremental Development of LOFAR Space Weather, the aim of the project is to demonstrate the capabilities of LOFAR for space weather studies in an incremental way, starting with a single LOFAR station and a small fraction of LOFAR filler time.

IDOLS achieves immediate benefit for the ILT partners interested in space weather and for the hardware development/study for LOFAR, allowing the realization/study of the dual-beam capabilities in a progressive way and without the need of upgrading all stations (or large fraction of them) to start having scientific results and demonstrating/performing simultaneous astronomical observations while monitoring space weather. What we demonstrate here using core station 32 (CS_032) may then be expanded, including any station with dual beam capabilities.

IDOLS first light was recorded on 2022-04-13 and since then operated every day. An initial team was set up to prepare the observing strategies and allow IDOLS to observe in parallel of the regular LOFAR observing program. At the moment, IDOLS records dynamic spectrum of the Sun during daylight and ionospheric scintillation using CasA at night time. The data is recorded on CEP4, without interfering with the other observing programs. A dedicate pipeline was created in order to display the recorded data in real time.

In this talk, we will show examples of the data-sets, discuss the potential and the capabilities of the project and discuss the future developments.

A Comprehensive analysis on RSTN metric type II bursts and their association with space weather events in solar cycle 24

Bendict Lawrance, Yong-Jae Moon, Pooja Devi, Ramesh Chandra, Rositsa Miteva

In this study we compile a list of metric type II radio bursts using Radio Solar Telescope Network (RSTN), to study the occurrence, associations and relationship among different solar activity phenomena. The RSTN data is freely available from 4 worldwide stations like Learmonth, Palehua, Sanvito and Sagamore Hills. By careful visual inspection we have collected all the major metric type II bursts detected in the range of 25-180 MHz. The relationships between all metric type IIs with the solar eruptive events like flares, coronal mass ejections (CMEs) and solar energetic particles (SEPs) are studied and the preliminary results are presented and discussed. This type of study will be helpful to reveal the information of solar and space weather activities based on radio perspectives. The new catalog of metric type II and associated solar events will be made freely available to the solar scientific community in the near future.

Recent advances on solar radio burst emissions, eruptive phenomena, and geomagnetic storms associated with in-situ particles in solar cycles 23 and 24

Rositsa Miteva, Susan W. Samwel, Svetoslav Zabunov, Kostadinka Koleva, Momchil Dechev, Ramesh Chandra

We present the occurrences of radio bursts of type II, III, and IV in association with solar energetic protons and electrons during solar cycles 23 and 24 (1996-2019). The comparative analysis shows more proton-accompanied type II radio bursts in the interplanetary space compared to the electron-related sample, whereas types III and IV radio bursts have the same occurrence rates. Recent advances in the analyses of solar flares of GOES X and M-class are also presented, in relation to other eruptive phenomena with a focus on their space weather relevance. Finally, we summarize the results of strong geomagnetic storms (Dst index amp<-100 nT) and their association trends over the last two solar cycles.

Posters session

See the list of poster abstracts.

Wednesday, September 28th

Session 9 - 09:00 – 10:45 – Planetary: Saturn

Session Chair: Ulrich Taubenschuss

[Invited] Magnetospheric dynamics revealed by the low-frequency radio components at Saturn

Siyuan Wu, Shengyi Ye, Georg Fischer, Ulrich Taubenschuss, Caitriona M. Jackman, Jian Wang, Elizabeth O'Dwyer, Baptiste Cecconi, William S. Kurth, John D. Menietti, Minyi Long, Shuo Yao ,Zhonghua Yao, Ruilong Guo, and Yan Xu

By analyzing the 13-year Cassini Saturn Orbital data measured by the Radio and Plasma Wave Science (RPWS) instrument, the complete spatial distribution and polarization features of Saturn narrowband emissions are obtained. Observation cases suggest that L-O mode 5-kHz narrowband emissions (NB) from Saturn can be reflected by the magnetosheath during solar wind compressions, leading to depolarization and trapping of NB inside Saturn's magnetosphere. The upper frequency limit of trapped NB depends on the plasma density in the magnetosheath, which is controlled by the upstream solar wind condition. A new radio component namely the Saturn Anomalous Myriametric Radiation (SAM), which is usually observed in a similar frequency range of the narrowband emissions and after the low-frequency extension of the Saturn Kilometric radiation, is discovered and their characteristics are summarized. SAM shows a possible connection to the solar wind compression of the magnetosphere. Based on an event list of the narrowband emissions, the rotational modulation analysis of the SKR, 5 kHz and 20 kHz narrowband emissions are carried out. The relative phase differences between the different radio components reveal a "phase lock" relation, suggesting these 'clock-like' emissions are triggered at different local times and in sequence of the phase relation. These results provide new insights to the large-scale Saturnian magnetospheric dynamics where the physical processes triggering these radio emissions take place sequentially in phase-locked pattern.

A special form of low-frequency cutoff of Saturn kilometric radiation

G. Fischer, U. Taubenschuss, D. Pisa, L. Lamy, S. Wu, and S.-Y. Ye

We studied the spectral morphology of Saturn kilometric radiation (SKR) with the Cassini RPWS (Radio and Plasma Wave Science) instrument and found a special structure at low frequencies which we nicknamed "caterpillar" due to its special shape and look in dynamic spectra. In this presentation we want to present the main physical characteristics of these newly identified form of SKR low-frequency cutoff emission. Caterpillars are coarse SKR structures lasting for several hours which have a constant central frequency mostly below 40 kHz and a typical bandwidth of about 10 kHz. The latter feature makes them easily distinguishable from Saturn narrowband emissions. Some of the caterpillars are connected to the main SKR emission at higher frequencies and some not. Their polarization is often similar to the one of the main SKR emission, but their total polarization degree is mostly lower. We found about 600 caterpillar emissions throughout the Cassini mission, and they were preferentially observed from beyond a distance of 10 Saturn radii in the equatorial plane or at lower latitudes. At high time resolution caterpillars show a smooth spectral structure, only the so-called striations were sometimes found superimposed above them.

A statistical view of the response of Saturn's radio emissions to solar wind driving

C.M. Jackman, C.K. Louis, A.R. Fogg, J.E. Waters, E.P. O'Dwyer, L. Lamy, M.F. Thomsen, T.M. Garton

Saturn has several components to its radio emission which can change in response to varying solar wind and magnetospheric conditions. These radio components include the Saturn Kilometric Radiation (SKR), a cyclotron maser instability-generated emission which occasionally displays Low Frequency Extensions (LFEs); and the Saturn narrowband emissions, typically below 40 kHz, which include n-SMR (narrowband Saturn Myriametric Radiation) and n-SKR. We utilize a list of all magnetopause and bow shock crossings by Cassini during its 13-year tour of the Saturn system [Jackman et al., 2019] to select out times when the Cassini radio (RPWS) instrument was sampling Saturn's radio emissions from the solar wind, magnetosheath and outer magnetosphere regions. We explore the hypotheses that the SKR is a good proxy for solar wind driving, and that narrowband emissions may link to dramatic magnetospheric reconfiguration events. We track the timeline between solar wind compressions observed during extended solar wind intervals and the occurrence of out-of-phase SKR bursts and LFEs (selected using a bespoke tool from Empey et al., 2021). Furthermore, we use boundary crossings in concert with magnetopause and bow shock models [Kanani et al. 2010; Went et al. 2011] to infer upstream solar wind dynamic pressure (DP) and pinpoint rapid large changes in DP which may indicate strong compressions – and their associated link to distinct radio signatures.

Testing the relationship between Saturn's ENA and narrowband SKR emissions

Joe Kinrade, Sarah Badman, Chris Paranicas, Caitriona Jackman, Diego Moral Pombo, Elizabeth O'Dwyer, Corentin Louis, Alexander Bader

Saturn's kilometric radio (SKR) and energetic neutral atom (ENA) emissions are important remote diagnostics of the planet's magnetospheric dynamics, intensifying during periods of global-scale plasma injection, and displaying characteristic planetary-period modulation. Here we analyse narrowband SKR (nSKR) emissions between 5-40 kHz, thought to originate near density gradients at the edges of the plasma torus. We test the hypothesis that nSKR production might be enhanced by inward-moving plasma following global plasma injection events. Global-scale ENA signatures have been associated with both 5 and 20 kHz nSKR emissions, particularly at dusk-sector local times where plasma injections are expected to have moved inwards through the magnetosphere, possibly triggering interchange instabilities.

We use a new set of calibrated equatorial ENA projections - captured by the Cassini INCA - to test the relationship between Saturn's ENA and nSKR emissions. The nSKR emission intensity peak often coincides with the rotation of ENA enhancement through the dusk local time sector. We test for radial distance dependence by constraining ENA keograms over a set of distances and local time sectors covering the edges of the plasma torus, and quantify the relative timing of nSKR enhancements through time-lagged correlation of the ENA intensity with flux density in the 5 and 20-40 kHz emission bands. We also observe periods of strong 5 kHz SKR emission when the ENA emission is absent, even during times of favourable viewing, indicating that this relationship is complex. These results contribute to our developing picture of how global plasma injection events can influence Saturn's inner magnetosphere, linking together two valuable observations of remotely-sensed global emissions, the ENAs and SKR.

Machine Learning for the Classification of Low Frequency Extensions of Saturn Kilometric Radiation

E.P O'Dwyer, C.M Jackman, K. Domijan and L. Lamy

Saturn Kilometric Radiation is an auroral emission that occurs between a few kHz to 1.2MHz, and peaks in the frequency range 100-400 kHz. It was detected quasi-continuously by Cassini from its arrival at Saturn in 2004 until mission end in 2017 and its properties have been extensively studied. SKR bursts which are global intensifications of SKR as well as extensions of the main SKR band down to lower frequencies, known as Low Frequency Extensions (LFEs), result from internally-driven tail reconnection and from solar wind compressions of the magnetosphere, which also trigger tail reconnection. LFEs have been selected by eye and also using a numerical criterion based on an intensity threshold [Reed et al., 2018]. In our work we propose to develop a supervised machine learning algorithm to select SKR bursts with an associated LFE from the entire Cassini dataset. The algorithm will be built using data from the Cassini radio instrument (RPWS), with LFEs selected by eye using a polygon selector tool by Empey et al., 2021 [zenodo.5636922] and will include examples of LFEs detected from a broad range of spacecraft locations. We plan to explore different types of algorithms that may be based on images, or on time series data e.g RNN, CNN, U-Net. We tried both a FFNN and a CNN to classifiy images of isolated LFEs and achieved preliminary testing accuracies of 89% and 87% respectively. Currently, we are using the U-Net model to generate a mask for images of isolated LFEs, allowing us to retain the shape (for interpretation of their frequency structure and its associated links to radio source location).

Electron solitary waves observed during the SKR source crossings by the Cassini Wideband receiver

David Pisa, Ulrich Taubenschuss, Georg Fischer, Jan Soucek, and Ondrej Santolik

Before the Cassini mission ended in late 2017, the spacecraft performed regular crossings of high latitude regions where Saturn kilometric radiation (SKR) is generated. SKR was continuously monitored by the Cassini-RPWS High-Frequency Receiver (HFR) but also in more detail by the Wideband Receiver (WBR) which recorded wave snapshots in the burst mode. Previous analyses from the SKR sources regions show the fine structures in SKR. Several studies from the terrestrial auroral regions show the presence of electron solitary waves (ESW) and discuss their relations to the fine structure of the radio emissions. We present WBR observations of ESWs obtained during Cassini's Grand Finale orbits while the spacecraft was within or very close to the SKR source region. We discuss the ESW properties, occurrence, and relation to observed SKR.

Session 10 - 11:15 – 12:30 – Exoplanets

Session Chair: Laurent Lamy

[Invited] Hunting for radio flashes from stars, brown-dwarfs and exoplanets

Vedantham, Harish

Low frequency (< few hundred MHz) radio observations uniquely probe several processes that determine the habitability of exoplanets such as coronal mass ejections and exoplanet magnetospheres. Radio observations of such phenomena in the solar system are commonplace. I will argue that the extrasolar frontier is now also within reach thanks to powerful new low-frequency telescopes such as LOFAR. I will describe an observational program using LOFAR to systematically survey the low-frequency radio sky for stellar, brown dwarf and exoplanetary emissions with unprecedented sensitivities. I will present some early successes of this campaign including (a) the discovery of evidence for magnetic interaction between a star and its planet (b) the discovery of a cold brown dwarf directly in the radio band using its magnetospheric emissions and (c) solar-type radio bursts on nearby stars possibly associated with coronal mass ejections. I will end with an outlook for harnessing radio astronomy's unique diagnostic capabilities to advance exoplanet science.

Stellar and exoplanetary radio emissions with LOFAR detected via multi-objects dynamic spectroscopy

Philippe Zarka, Cyril Tasse, Alan Loh, Emilie Mauduit, Jake Turner, Laurent Lamy, Jean-Mathias Grießmeier, Joe Callingham, Harish Vedantham, & the Exoradio team

After a brief review of LOFAR results to date on exoplanetary and stellar radio emissions, I will present a new detection method: the multi-objects dynamic spectroscopy (MODS), well adapted to the detection of slow radio transients. It consists in computing, as an end product of the LOFAR imaging pipeline, from the residual visibilities, a dynamic spectrum for any point of the observed field. We have provided to the LOFAR surveys team an input catalog of exoplanets and stars, from which ~32500 dynamic spectra have been produced as well as twice as many dynamic spectra on random "Off" positions, in the frame of the LOFAR 2-meter Sky Survey (LoTSS). I will present, as a result of the statistical analysis of these ~100000 dynamic spectra, evidence for the detection of a few tens of stellar targets and a few exoplanetary targets at frequencies around 150 MHz, as well as examples of their dynamic spectra. These targets will feed the input catalog of targets for the NenuFAR Exoradio large program, that will perform extensive follow-up observations, also making use of the MODS methodology.

Follow-up observations of the first possible exoplanet radio detection

Jake D. Turner, Philippe Zarka, Jean-Mathias Grießmeier

Many of the discovered exoplanets are unlike our Solar System planets. Characterizing these alien worlds offers insights into planet formation, planetary system architectures, and even the possibility of planetary habitability. Astronomers have developed a variety of techniques to probe their radii, masses, temperatures, orbital parameters, and atmospheric compositions. However, one of the most important planetary properties is not yet directly detected despite decades of searching: the presence of a magnetic field. Observing planetary auroral radio emission is the most promising method to detect exoplanetary magnetic fields. All of the gas giants planets in our Solar System have a magnetic field, and theoretical studies predict that many exoplanets should as well. Observations of exoplanet magnetic fields would yield constraints on planetary properties difficult to study, such as interior structure, atmospheric escape, and star-planet interactions. Magnetic drag could be an important factor in the dynamics of exoplanetary atmospheres. Additionally, magnetic fields may contribute to the sustained habitability of terrestrial exoplanets.

Recently, we published the first possible detection of an exoplanet in the radio (Turner et al. 2021). We observed the exoplanetary system tau Boo using LOFAR beamformed observations. We tentatively detected slowly variable and bursty emission from 14-30 MHz. Assuming the emission is from the planet, we derived a maximum surface polar magnetic field for tau Boo b between ~5-11 G. The magnetic field and emission strengths we derived are consistent with theoretical predictions, and if this detection is confirmed it will place important constraints on dynamo theory. However, the source of these tentative signals are still uncertain and follow-up observations are needed to confirm our detections.

In this talk, we present the first results of an extensive multi-site follow-up campaign to confirm the radio detection of tau Boo b. Our campaign consists of low-frequency beamformed radio data from 15-62 MHz taken simultaneously from NenuFAR and LOFAR. Additionally, we monitored the stellar light curves for stellar flares simultaneously with Evryscope and partially with TESS. The observations cover most of the orbit multiple times to search for periodicity of the detected signal. Preliminary analysis of the data show no signs of slow emission. Therefore, the original signal may have been caused by an unknown systemic or we are observing variability in the planetary radio flux due to observing at different parts of the stellar magnetic cycle. Preliminary results of the slow emission will also be discussed. Analysis of the data is still ongoing.

Required conditions for an exoplanet to emit radio waves and implications for observational campaigns

J.-M. Grießmeier, N. V. Erkaev, C. Weber, H. Lammer, V. A. Ivanov and P. Odert

The detection of radio emission from an exoplanet would constitute the best way to determine its magnetic field. Indeed, the presence of a planetary magnetic field is a necessary condition for radio emission via the Cyclotron Maser Instability. The presence of a magnetic field is, however, not sufficient. At the emission site, the local cyclotron frequency has to be sufficiently high compared to the local plasma frequency. The plasma frequency depends, in turn, on the planetary mass, its orbital distance, and its host star. We will discuss in which cases radio emission can be generated efficiently. We will present implications for the target selection for observation campaigns and consequences for the interpretation of observational data.

Session 11 - 14:00 – 15:15 – Exoplanets & Interplanetary
Session Chair: Carine Briand

Exoplanet radio search with NenuFAR

Emilie Mauduit, Philippe Zarka, Jean-Mathias Griessmeier, Alan Loh

The radio detection of exoplanets will considerably expand the field of comparative magnetospheric physics and star-planet plasma interactions [1]. It will be a topic of interest for the future SKA radiotelescope [2]. It has been convincingly argued that magnetospheric radio emissions, of cyclotron origin, should preferably occur at low frequencies [3]. The new radiotelescope NenuFAR [4], a pathfinder of SKA, will provide exceptionally high sensitivity at the lowest radio frequencies observable from the ground, between the ionospheric cutoff (10 MHz) and the radio FM band (87 MHz). But still, the very bright galactic background, intense radio interference, and propagation and instrumental effects in this spectral range make it very difficult to detect weak broadband signals without any characteristic time-frequency signature (dispersion, short-term period, narrow spectral lines…) as exoplanetary radio signals are expected to be.

We are thus defining a strategy that will maximize the capability of detection of an exoplanetary radio signal with NenuFAR. This strategy is based on preparatory studies including (1) the construction of an up-to-date and evolutive target catalog, based on observed exoplanet physical parameters, radio emission theory, and magnetospheric physics (embedded in scaling laws) [5,6], and (2) the temporal and spectral optimization of the observations scheduling and analysis, based on (2a) statistics of the NenuFAR radio interference environment, (2b) the modelization of the time-dependent contamination of observations by unwanted signals from strong radio sources (Jupiter, Sun, A-team) entering the radiotelescope grating or side lobes, and (2c) an homogeneous – and massive – coverage of the orbital phases of the exoplanetary target relative to its parent star.

Data analysis will heavily rely on interference and contamination elimination, and also detection of circularly polarized signals. These signals modulation at the exoplanet's orbital period will be the smoking gun evidence of their origin.
I will present the results of the above preparatory studies, as well as an example of the end-to-end processing of observations of one target.

Detecting Beamed Radio Emission from Exoplanets

Reza Ashtari, Anthony Sciola, Jake Turner

Radio observation of planetary auroral emission provides unique and complementary insight toward planetary science not available via orthodox exoplanet observation techniques. Providing the first measurements of planetary magnetic fields, rotation and obliquity, we gain necessary and crucial insight towards our understanding of the star-planet relationships, planetary interiors, and habitability of exoplanets. Using a stellar-wind driven Jovian approximation, we present analytical methods for estimating magnetospheric radio emission from confirmed exoplanets. Predicted radio fluxes from cataloged exoplanets are compared against the wavelength and sensitivities of current and future observatories. Candidate exoplanets are down-selected based on the sky coverage of each ground-observatory. Orbits of target exoplanets are modeled to account for influential orbital-dependent effects in anticipating time-varying exoplanet radio luminosity and flux. To evaluate the angular alignment of exoplanetary beamed emission relative to Earth's position, the equatorial latitude of exoplanetary auroral emission is compared against Earth's apparent latitude on the exoplanet. Predicted time-dependent measurements and recommended beamformed observations for ground-based radio arrays are provided, along with a detailed analysis of the anticipated emission behavior for tau Boo b.

The null detection of exoplanetary radio emission: Role of seed magnetic field structure of primordial origin

K. M. Hiremath

Expected radio emission from the extra solar planets due to physical phenomenon called "electron-cyclotron maser instability" (ECMI) requires two necessary conditions: right magnitude of velocity of stellar wind and existence of magnetic field structure of the planet. Assuming that stellar wind exists, in this study, we probe the second necessary condition for the existence of magnetic field structure. One scenario for existence of magnetic field structure of planets is due to "dynamo mechanism" for which Lorenz and Coriolis forces are of similar orders is required. Importantly, to excite and generate such a dynamo, a large-scale (at least of the dimensions of planets) seed magnetic field structure of primordial origin, that might have been retained from the early history of star and planetary formations, is required. We surveyed all the radio observations of exoplanets and found that most of the observed planets are of dimension of solar Jupiter. In order to verify the existence of seed magnetic field, we compute the magnetic diffusion time scale which is a function of dimension of the object, magnitude of magnetic 38iffusivity and a coefficient that depends upon the boundary conditions. For all the exoplanets considered for radio observations, we estimate magnetic diffusion time scales which are found to be ~ few million years and existence of exoplanetary magnetic field structure upto present age is questionable. The only way to circumvent this problem is dynamo generated magnetic field structure which some how might have been generated without seed magnetic field structure. Unfortunately having a dynamo generated magnetic field structure appears to be unlikely as many extrasolar planets have null detection of observed radio emission due to ECMI. Coming back to scenario of seed magnetic field structure, with the present instrumental sensitivity limits, one has to expect statistically significant radio emission for the planets whose host stars must have ages of ~ few million yrs old or less that rotate fast.

Plasma Densities Measured in the Very Local Interstellar Medium

W. S. Kurth, L. J. Granroth, L. F. Burlaga, and S. D. Bale

A fundamental property of the Very Local Interstellar Medium (VLISM) is the number density of electrons, or electron plasma density. The Voyager Plasma Wave Science (PWS) Instrument has provided the only in situ measurements of this parameter, to a heliocentric distance of 155 AU. As predicted in the early 1990's, Voyager has occasionally observed electron plasma oscillations in the foreshocks of shocks related to solar transients that propagate all the way through the heliosphere over time scales of hundreds of days. These emissions occur at the local electron plasma frequency that is directly proportional to the square root of the electron density. Voyager 1 has detected eight plasma oscillation events at a rate of roughly one per year. Voyager 2 has detected three such events. Combined, the Voyager 1 and 2 density measurement show a large-scale radial gradient beyond the heliopause, within 10's of degrees of the nose of the heliosphere. Since about 2016, a narrow, weak line at the plasma frequency has been detected using special processing of the high spectral resolution waveform

measurements on Voyager 1. These emissions appear without the existence of Intense plasma oscillations, hence, provide more continuous density measurements. It is thought that this emission is related to a Maxwellian distribution combined with a Kappa distribution with K ~ 1.53. This line and serendipitous observations of plasma oscillations has made it possible to measure the density change across some shocks and pressure fronts observed in the magnetic field by the Voyager magnetometer. In cases where both the density and |B| changes are measured, the ratios of the changes in these quantities compare quite favorably and allow the study of these transient features in the VLISM.

Session 12 - 15:45 – 17:00 – Instrumentation

Session Chair: Rosita Miteva

Single-Dish Solar Radio Imaging with INAF Radiotelescopes

A.Pellizzoni on behalf of the SunDish collaboration [online]

We present a new solar radio imaging system implemented through the upgrade of the large single-dish telescopes of the Italian National Institute for Astrophysics (INAF), not originally conceived for solar observations (https://sites.google.com/inaf.it/sundish).
During the development and early science phase of the project (2018-2020), we obtained about 170 maps of the entire solar disk in the 18-26 GHz band, filling the observational gap in the field of solar imaging at these frequencies. These solar images have typical resolutions in the 0.7-2 arcmin range and a brightness temperature sensitivity <10 K. Accurate calibration adopting the Supernova Remnant Cas A as a flux reference, provided typical errors <3% for the estimation of the quiet-Sun level components and for active regions flux measurements.
As a first early science result of the project, we present a catalog of radio continuum solar imaging observations with Medicina 32-m and SRT 64-m radio telescopes including the multi-wavelength identification of active regions, their brightness and spectral characterisation. The interpretation of the observed emission as thermal bremsstrahlung components combined with gyro-magnetic variable emission paves the way to the use of our system for long-term monitoring of the Sun. We also discuss useful outcomes both for solar physics (e.g. study of the chromospheric network dynamics) and space weather applications (e.g. flare precursors studies).

AERO-VISTA: Vector sensor mapping of the Earth's auroral radio emission with twin 6U CubeSats [online]

Philip J. Erickson, Frank D. Lind, Mary Knapp, Rebecca Masterson, Frank C. Robey. James LaBelle, Allan Weatherwax, David G. McGaw, Geoffrey Crew, John Swoboda, Ryan Volz, Ekaterina Kononov, Lenny Paritsky, Erik Thompson, Mark Silver

Earth's aurora has a complexity and richness in both energetics and spatial / temporal structure that is of intense interest for our understanding of space physics. Auroral radio emissions from the ionosphere in the 400 kHz to 5 MHz range are a powerful space physics tool because they provide a means to remotely sense auroral ionospheric plasma conditions and processes. The Auroral Emission Radio Observer (AERO) and Vector Interferometry Space Technology using AERO (VISTA) comprise AERO-VISTA, a 90-day twin CubeSat mission in low Earth sun synchronous polar orbit that will qualify and validate a novel electromagnetic vector sensor. AERO-VISTA will answer key scientific questions about the nature and sources of auroral radio emissions, including AKR, roar, hiss, and mid-frequency bursts, that cannot be addressed from the ground due to shielding by the ionosphere.
AERO-VISTA is on schedule for delivery of flight hardware after the summer of 2022. In this presentation, we will describe the science goals of the AERO-VISTA mission, the design of the spacecraft and payload, discuss vector sensor sensitivity and direction-finding capability based on lab data, and present recent flight model radio test results.

TFCat, a Spectro-Temporal Feature Catalogue format

Cecconi, B; Bonnin, X.; Loh, A.; Taylor, M.

Low frequency radio astronomy features are primarily identified through their spectra-temporal shape. Many event catalogues have been published since the early ages of radio astronomy, but no standard emerged yet making it difficult to process and reuse those catalogues.

We have developed a flexible catalogue format, derived from GeoJSON, a standard for geo-referenced feature catalogues on Earth and planetary surfaces. We present the case for this new catalogue format, together with published catalogues examples. We also show how this format facilitates the reuse of the catalogues.

An Advanced Low-band VHF Radar Observatory for Solar, Space Weather, Planetary, and Astronomical Research

Brett Isham, Jason Kooi, Namir Kassim, Joseph Helmboldt, Jorge Chau, Juha Vierinen, Michael Nolan, Michel Blanc, Wlodek Kofman

The construction of a low-band VHF radar observatory -- for research spanning the solar corona and solar wind; geospace including the magnetosphere, ionosphere and neutral atmosphere; and the moon, planets, asteroids, and meteors -- has been a decades-long dream of space scientists. Studies of exoplanets, interplanetary scintillation, and other passive radio astronomical observations would also be possible.

Over the years our awareness of what might be gained by such an observatory has increased, and the techniques that can be used have dramatically improved, making this an opportune time for the design and construction of a powerful and capable modern radar observatory.

Possibilities for solar radar observations will be presented as an example of the potential of the proposed system for achieving selected science goals. Solar radar will be a game changer for solar physics research and space weather prediction and monitoring, including early warning of earth-directed coronal mass ejections. Space weather is a critical factor in communication, navigation, power distribution, and for both manned and unmanned aircraft and spacecraft.

Before the collapse of the Arecibo Observatory instrument platform in December 2020, Arecibo Observatory was a part of the American radar chain and the 60W/120E great circle initiative. The potential incorporation of a low-band VHF radar together with a renewed Arecibo Observatory could be a benefit to Arecibo and the radar chain, and to solar, heliospheric, and geospace science.

Posters

Solar

Poster #1

Interferometric imaging of the type IIIb and U radio bursts observed with LOFAR

Dabrowski, B

We present the LOFAR observations, in the frequency range of 20-80 MHz, of the type IIIb and U solar radio bursts which appeared on 22 August 2017. We study their source size and evolution in different altitudes, as well as the velocity and energy of electron beams responsible for their generation. Additionally to LOFAR observations, we use the data recorded in the EUV (from SDO) and in X-ray spectral ranges (from GOES and RHESSI). Our study shows that the LOFAR observations, in combination with observations at other wavelengths can give better understanding of the physical processes responsible for type IIIb and U solar radio bursts generations.

Poster #2

A new L-S solar flux radio telescope and its recently observation results

Dong, L.

We build a solar radio telescope located in Lang fang City He bei Province—39°23'N,116°39'E . It has 8 independent 5MHz monitoring frequency bands and there are 16 Channels with two polarizations from L band to S band which respectively are 1230MHz, 1320MHz, 1380MHz, 1426.8MHz, 1520MHz, 1600MHz, 1650MHz, 1695MHz, 2840MHz.

During nearly 4 months continuously observation, we find that the solar flux of 2840MHz has a good correlation with the real time X-ray solar flux in short time, and sunspot Area in long time. In our poster, we will show you some observation results such as the solar radio bursts comparing the X-ray data from GOSE in short time, and the long time F10.7 index variation comparing international index by space weather Canada

Poster #3

Fine structure of a solar type III radio bursts observed with LOFAR

Wołowska, A.

We report high frequency and time resolution LOFAR observations in the frequency range of 20-80 MHz, of the type III solar radio bursts which appeared on 8 April 2019. They are accompanied by different fine structures appearing in 20-40 MHz range.

We have prepared dynamic spectra produced with the use of LOFAR Solar Imaging Pipeline, and classified the observed phenomena to several generally accepted groups of fine structures.

We also discuss their properties, such duration, spectral width, drift and general statistics of the whole sample.

Poster #4

Solar Radio Observations at high spectral and temporal resolution with NenuFAR

C. Briand, P. Zarka & ES11-team

NenuFAR is a large low-frequency radio-telescope recently deployed in France. It is a standalone phased array and interferometer, as well as a low-frequency extension of LOFAR. It covers frequencies between 10 and 85 MHz. Its large collecting surface (~53000m^2 at 25MHz) makes it very sensitive. Spectral and temporal resolution can be very high, respectively, down to δf=0.1kHz and/or δt=0.3ms (with a limitation at $\delta f \times \delta t \geq 4$). Such resolutions, associated with high sensitivity, is unique at low frequency. Each antenna is composed of two crossed dipoles allowing polarization measurements in the four Stokes parameters.

Solar observations were performed during the Early Science phase, in particular since December 2021. Many Type III bursts were recorded, some with exceptional fine structures as stria or slowly drifting emission, others with a very weak signal, Type II emissions with highly polarized herringbones were detected too. The capabilities of NenuFAR observations with such high resolution and polarimetric modes are presented. At the beginning of the solar cycle 25, the instrument provides unprecedented possibilities to study the solar corona.

Poster #5

Type III solar radio burst masking using convex hulls and uniform subdivision

M. B. R. Amin, R. Flynn, E. Carley, P. Gallagher, M. Daly

Coronal Mass Ejections (CMEs), Solar flares, and sunspots have powerful radio emissions associated with them. These emissions, known as Solar Radio Bursts (SRBs), are one of the most extreme space weather events in our solar system. Given the effect SRBs can have on orbiting satellites, ground based power infrastructure, and terrestrial weather, their successful detection and classification in a timely manner has become imperative. However, classifying SRBs has become a complex computational challenge in recent years with the significant volume of data that is collected daily from advanced radio telescopes such as the Low Frequency Array (LOFAR) and that thousands of SRBs can occur per day. In recent years, computer vision techniques have been applied to detect and classify SRBs in these large datasets with considerable success using Convolutional Neural Networks (CNNs) via YOLO (You Only Look Once). There are issues with the detections of SRBs with these methods, most notably the bounding box Region of Interest (ROI). In this research, as a precursor to adapting the SRB detection/classification problem to a mask-RCNN system, the Graham Scan and DLG uniform subdivision algorithms have been chosen to create a mask for Type III SRBs with a view to extending this method to Type II. Results have shown that, unlike standard edge detection and contour algorithms which make no distinction of any artefact in an image, the combination of Graham Scan and DLG produces a bounding mask in the ROI determined by a few reference points. Using the convex hull algorithm avoids any loss of information when the uniform subdivision interpolates between references points to produce a final masked ROI.

Poster #6

Imaging-spectroscopy of a band-split type II solar radio burst with the Murchison Widefield Array

Shilpi Bhunia, Eoin Carley, Divya Oberoi, Peter Gallagher

Type II solar radio bursts are believed to be caused by magnetohydrodynamics (MHD) shock-accelerated electrons in the solar corona. Often type IIs exhibit fine structures in their dynamic spectra. For example, both fundamental and harmonic bands of type II bursts are split into two sub-bands. This is generally believed to be coming from upstream and downstream regions of the shock; however, this explanation remains unconfirmed. Here we present results from imaging analysis of type II radio burst band-splitting and fine structures observed by the Murchison Widefield Array (MWA) on 2014-Sep-28. The MWA provides high-sensitivity imaging spectroscopy in the range of 80-300 MHz with a time resolution of 0.5 s and a frequency resolution of 40 kHz. Our analysis provides rare evidence that band-splitting is caused by emission from multiple parts of the shock (as opposed to the upstream/downstream hypothesis). We also examine the small-scale motion of type II fine structure radio sources in MWA images. We suggest that this small-scale motion may arise due to propagation effects from coronal turbulence, and not because of the physical motion of the shock location. The study of the systematic and small-scale motion of fine structures may therefore provide a measure of turbulence in different regions of the shock and corona.

Solar / heliospheric / Space Weather

Poster #7

Ionospheric Plasma Fluctuation RESPONSE to space weather events in September 2017, August 2018 and March 2015 (St Patrick's day) over the Equatorial and Low Latitude ionosphere.

Patrick Essien, CAD Figueirido, H. Takahashi, C. M. Wrasse, N. K. B. Klutse, S. O. Lomotey, R. Babatunde

Using data collected by GNSS dual frequency receivers' network, detrended TEC maps were generated to identify ionospheric plasma fluctuations with characteristics of medium-scale traveling ionospheric disturbances (MSTIDs) over the South American equatorial region during space weather events. During the September 2017, August 2018 and March 2015 (St Patricks day) geomagnetic storm, MSTIDs were observed especially during daytime and sometimes initiate equatorial plasma bubble even though those seasons are not favourable for the generation of the bubbles. The present work serves as a strong foundation to unearth the mystery of ionospheric TIDS during space weather events and consequently the contribute to the global ionospheric weather.

Poster #8

Total Electron Content Variation during a HSS/CIR driven storm in High and Middle Latitudes

Prasannakumara Pillai Geethakumari

Magnetic storms are caused by the interactions between the solar wind and the Earth's magnetosphere. Many studies were carried on strong magnetic storms. However, moderate storms and their impacts on the ionosphere are less explored. This study investigates the large-scale and mesoscale structures in ionospheric total electron content (TEC) during a moderate storm (the sym_H index minimum: -63 nT) driven by solar wind high-speed streams (HSSs). For the solar wind, the IMF Bz was down to -20 nT and the solar wind speed up to 612 km/s. The GNSS/TEC maps are obtained from the Madrigal database. The associated field-aligned currents (FACs) from Active Magnetosphere and Planetary Electrodynamics Response Experiment (AMPERE), ionospheric convections from Super Dual Auroral Radar Network (SuperDARN), and the O/N2 ratio from TIMED/GUVI are also studied for understanding the physics behind.

Our analysis shows the different responses of TEC during the storm initial, main, and recovery phases. During the initial phase, weak meso-scale TEC structures (enhancement and depletion) are found mainly at high latitudes within the auroral oval and close to the cusp, plausibly associated with the enhancement of FACs. After the onset of the main phase, the TEC are enhanced at mid- and low-laittudes with a maximum of ~10 TECU. During the main phase, we observed the evolution of a storm-enhanced-density (SED) plume in the American sector and a transient enhancement of TEC in the polar cap. During the late main and the recovery phases, strong TEC depletion at mid-and high- latitudes is found on the dayside in the American sector. The depletion is highly associated with the decrease of the O/N2 ratio. The possible physical mechanisms will be discussed.

Poster #9

Probing the response of the D-region ionosphere to solar flares and associated geomagnetic activity over Ireland

Victor U. J. Nwankwo, Catriona Jackman, Peter Gallagher, and Sophie Murray

We probe the spaciotemporal variability of the lower ionosphere driven by solar flares and associated geomagnetic disturbances, using very low frequency (VLF) narrowband measurement (from different transmitters) and collocated ground-based magnetometers. The sites of the VLF receiving stations are located at Birr (Ireland), Dunsink Observatory (Ireland) and Muret (Southern France). We thus investigate the physical processes in the D-region ionosphere in response to flare-induced X-ray flux enhancement and associated perturbation of geomagnetic field along multiple propagation paths, referencing the Ireland regions.

Poster #10

Detection of Solar radio bursts at Mars

Beatriz Sanchez-Cano, Mark Lester, Simon Joyce, Samuel Carter, Sophie Musset, Baptiste Cecconi

The Sun emits radio waves that propagate through the solar corona and interplanetary medium, where they are refracted and scattered. One of the most intense radio sources in the kilometric range are the solar type III radio bursts, which are associated with solar flares and are produced when the Langmuir waves are excited by the flare accelerated electron beams that propagate along open magnetic field lines. These radio bursts are typically detected by instruments operating in the radio frequency and are identified as sudden bursts in which their emissions drift rapidly from high to low frequencies in a very short amount of time (of the order of seconds-minutes).

Solar type III radio bursts have been studied since the forties but all observations were limited to Earth's orbit. Recently, more information is being gather thanks to new solar missions such as Solar Orbiter and Parker Solar Probe. However, our knowledge at Mars' orbit remains limited. In this study, we explore the near 17 years of Mars Advanced Radar for Subsurface and Ionosphere Sounding (MARSIS) onboard Mars Express, which has been regularly recording these radio bursts since its deployment at Mars in mid-2005. We will show the observation that we have at Mars, as well as a first characterisation of these solar events, and when possible, we compare them with their solar source and with any other spacecraft in the Solar System detecting the same emissions.

Planetary

Poster #11

Observations of the First Harmonic of Saturn Kilometric Radiation during Cassini's Grand Finale

Siyuan Wu, Philippe Zarka, Laurent Lamy, Ulrich Taubenschuss, Baptiste Cecconi, Shengyi Ye, Georg Fischer, William S. Kurth, and Théo Francez

Clear first harmonic emissions of Saturn Kilometric Radiation are discovered during the Cassini Grand Finale orbits. Both O mode and X mode fundamental emissions accompanied by X mode harmonics are observed. Analysis shows that the frequency ratio between the fundamental and harmonic emissions is 2.01±0.08, and the harmonic emissions display weaker intensities than the fundamental, by more than 40 dB. The intensity relations between the two types of harmonics, i.e., O-X (fundamental-harmonic) and X-X show different patterns that we attribute to different conditions of emission at the source. Direction-finding results shows that the fundamental and harmonic emissions are plausibly generated in the same source region. In agreement with previous studies at Earth, the generation of the two types of harmonics can be attributed to the cyclotron maser instability operating with different plasma density and electron energy distributions in the source region.

Poster #12

Radio emissions induced by Uranus-moons interactions?

C. K. Louis, L. Lamy, C. M. Jackman, B. Cecconi

Several of Jupiter's and Saturn's moons are known to induced Ultraviolet (UV) auroral emissions at the footprint of their magnetic flux tube [Prangé et al., 1996, Clarke et al., 1998, Clarke et al., 2002, Pryor et al., 2011]. At Jupiter, the Galilean moons Io, Europa and Ganymede are also known to be responsible for powerful decametric radio emissions [Bigg, 1964, Louis et al., 2017a, Zarka et al., 2018]. Like the rest of auroral radio waves, these moon-induced radio emissions have been shown to be driven by the Cyclotron Maser Instability from loss cone electron distributions functions of a few keV [Hess et al., 2008, Louis et al. 2020]. At Uranus, Kistler (1988) attributed the periodic signature of a kilometric radio emissions seen by Voyager 2/PRA to a similar alfvenic interaction between the moon Ariel and the planet. Therefore, in the context of preparing a future Uranus Orbiter, we present here simulations of the expected radio emission induced by the moons Ariel and Miranda, using the Exoplanetary and Planetary Radio Emission Simulator (ExPRES, Louis et al., 2019). We present a statistical parametric study of the expected Uranian moon-induced radio emission, by varying the inputs of the ExPRES code, such as the magnetic field models, the electron energy and distribution function, and the opening of the beaming angle. The simulations are compared to the Voyager 2/PRA high resolution data recently refurbished in a digital format [Cecconi et al., 2017].

Poster #13

Radio Emissions from Electrical Activity in Martian Dust Storms

Walid Majid

Dust storms on Mars are predicted to be capable of producing electrostatic fields and discharges, even larger than those in dust storms on Earth. There are three key elements in the characterization of Martian electrostatic discharges: dependence on Martian environmental conditions, event rate, and the strength of the generated electric fields. The detection and characterization of electric activity in Martian dust storms has important implications for habitability, and preparations for human exploration of the red planet. Furthermore, electrostatic discharges may be linked to local chemistry and plays an important role in the predicted global electrical circuit.

Because of the continuous Mars telecommunication needs of NASA's Mars-based assets, the Deep Space Network (DSN) is the only facility in the world that combines long term, high cadence, observing opportunities with large sensitive telescopes, making it a unique asset worldwide in searching for and characterizing electrostatic activity from large scale convective dust storms at Mars. We will describe a program at NASA's Madrid Deep Space Communication Complex that has been carrying out a long-term monitoring campaign to search for and characterize the entire Mars hemisphere for powerful discharges during routine tracking of spacecraft at Mars on an entirely non-interfering basis. The ground-based detections will also have important implications for the design of a future instrument that could make similar in-situ measurements from orbit or from the surface of Mars, with far greater sensitivity and duty cycle, opening up a new window in our understanding of the Martian environment.

Poster #14

Reconsideration for causalities of occurrence features of Jupiter's Io-related radio emission

Hiroaki Misawa, Atsushi Kumamoto and Rikuto Yasuda

The following questions; 'What kind of magneto-ionic wave Jupiter's auroral radio emission is?' and 'How the radio emission is generated?' have been long years of subjects. We have investigated the subjects particularly for Io-related decametric radio emission (Io-DAM) based on numerical calculations using several kinds of magnetic field and plasma density models, however, the questions have not been resolved yet: a hypothesis of some special energy transportations which do not meet with the observation results. Recently Jupiter's new magnetic field model was released based on the magnetic field observations near Jupiter conducted by the 'Juno' Jupiter explorer. We have tried to make a 3D ray-tracing analysis for Io-DAM using the new magnetic field model. The preliminary analyses show that R-X mode waves are preferable as Io-DAM and the new magnetic field model gives more natural explanations for the origin of Io-DAM, though there still remain some questions on restriction of Io-DAM.

Poster #15

Evidence of fresh injections related to the interchange instability in the Io torus

W. S. Kurth, G. B. Hospodarsky, A. H. Sulaiman, B. H. Mauk, G. Clark, F. Allegrini, J. E. P. Connerney, and S. J. Bolton

The Juno Waves instrument often detects brief, band-limited emissions when the spacecraft crosses magnetic fields threading Io's M-shell, or vicinity thereof, up to about 30 degrees magnetic latitude. The disturbances have durations of from several seconds to of order one minute and are observed below the electron cyclotron frequency. While plasma densities are often not available, it is thought that the events occur in a plasma regime in which the surrounding plasma frequency is above the frequency of the emissions. Often, there is a band just above the electron cyclotron frequency when these are observed, the first electron cyclotron half-harmonic, that is weakened or disrupted at the time of the events. While the events can be seen in isolation, there are typically a few of them with temporal spacing between about 15 to 40 minutes. Similar features were commonly seen by the Cassini radio and plasma wave instrument and were identified as ‘fresh’ injections or evidence of inward-moving flux tubes due to the centrifugal interchange instability. As such, they were characterized as having depleted thermal plasma and enhanced energetic plasma with electron distributions unstable to wave modes such as the upper hybrid band and chorus. As fresh injections, the energetic particles associated with them have not had time to drift in longitude due to gradient and curvature drift forces.

Poster #16

Satistical analysis of the jovian decametric emissions with the Nançay Decameter Array

H. R. P. Jácome, M. S. Marques, E. Echer, P. Zarka, L. Lamy, C. Louis

The extensive digital catalog of the Nançay Decameter Array (NDA) comprises all the daily observations of Jupiter, from ~10 MHz to 40 MHz, acquired by the Array since late 1990. Thanks to its large extension, the NDA catalog has provided statistical evidence of partial control of the Jovian decametric (DAM) radio emissions by the satellites Io, Europa and Ganymede. Besides, it is well suited for long term studies of Jupiter DAM variations. In this work, we present Europa-induced emissions detected from statistical analyses of the NDA catalog and an analysis of the dependence of Jovian DAM emissions’ measured characteristics on the Earth-Jupiter declination.

Poster #17

Fine and coarse spectral structures of Jovian kilometric radiation revealed by Juno and Cassini

G. Fischer, U. Taubenschuss, D. Pisa

Cassini flew past Jupiter in 2000/2001, and Juno is orbiting the gas giant since mid-2016. Here we focus on the spectral properties of Jovian kilometric radiation (KOM), which can take the form of a narrow-banded (nKOM) or a broad-banded (bKOM) emission. It is certain that bKOM is caused by the cyclotron maser instability, whereas nKOM might be caused by a mode conversion of upper hybrid waves at the boundary layer of the Io plasma torus. This might also lead to different spectral structures: While nKOM is very smooth and practically shows no fine structures, one can find zebra patterns and striations in bKOM. There are linear features of positive or negative slope in bKOM spectra which should rather be called "coarse" structures. Their typical bandwidth is some tens of kHz, and they last for some tens of minutes. We investigate the occurrence of these coarse bKOM structures with time and CML and distinguish between negatively and positively sloped ones.

Poster #18

Latitudinal Distribution of Auroral Kilometric Radiation based on POLAR spacecraft observations

Kevin D. Smith, Corentin Louis, Caitriona Jackman, Alexandra R. Fogg, James Waters, Elizabeth O’Dwyer, Larry Granroth

Auroral Kilometric Radiation (AKR) is a terrestrial radio emission that occurs above the poles. It is produced by the cyclotron maser instability at frequencies close to the electron cyclotron frequency (proportional to the magnetic field amplitude). The POLAR orbiter sampled radio emissions from pole to pole, thus AKR emissions were sampled across a broad range of latitudes. This is important because the frequency and visibility of AKR emissions depend on observer latitude. In order to distinguish AKR emissions from other radio sources we used the “SPectrogram Analysis and Cataloguing Environment” (SPACE) labelling tool to create a labelled catalogue. From this catalogue we derived occurrence and intensity distributions relative to frequency and observer latitude. These distributions allowed constraints to be put on the viewing effects and for the underlying physics of AKR emissions to be studied. Our results can be compared to simulations of AKR and to auroral radio emissions on other planets to put constraints on the characteristics of emissions and their propagation.

Poster #19

Numerical radar simulation for the explorations of the ionospheres of Jupiter’s icy moons

Rikuto Yasuda, Tomoki Kimura, Hiroaki Misawa, Fuminori Tsuchiya, Atsushi Kumamoto, Yasumasa Kasaba

Jupiter's icy moons such as Europa and Ganymede may harbor subsurface liquid water oceans and have ionospheres created from the oceanic water materials. While only Earth has the ocean on the surface in the current solar system, multiple icy bodies like the icy moons of giant planets have oceans in their subsurface under the icy crust. The icy bodies' oceans are potentially more universal habitable environment than the Earth-type surface ocean. Structures of the ocean and the ionosphere of the icy moons are essential information for understanding the universality of habitable environments. However, the structures of the oceans are unknown because in-situ or lander explorations on the surface of icy objects, the most effective method for exploring the structures, are still at technically conceptional level at present. The structures of ionospheres are still unclear as well because the ionospheric radio occultation and other effective explorations have difficulties of limited observing opportunities. There we have been trying to uncover the structures of the ocean and the ionosphere of Jupiter's icy moons by the radar exploration with the Radio & Plasma Wave Investigation (RPWI) and the Radar for Icy Moon Exploration (RIME) onboard the Jupiter ICy moons Explorer (JUICE). For the investigations of radio wave sounding in and around the icy moons with RPWI and RIME ranging in tens KHz to tens MHz, we have developed a numerical simulation code that models the propagation of electromagnetic (EM) waves and emulated occultation of the Jovian radio waves by the icy moon's ionospheric structures during the flybys of the Galileo spacecraft to Jupiter's icy moons. In this presentation, we will indicate derived vertical ionospheric profiles of Europa, Ganymede and Callisto exhibiting unique ionospheric characteristics. As the next step, we plan to simulate the reflection and transmission of the EM waves in the icy crust and underlying ocean. By combining this new simulation with our current one for the ionospheres, icy moon's ionospheric and subsurface structures are expected to be elucidated. These simulations would also give constrains on the pressure and temperature of the subsurface, which finally lead to deep understandings of the icy moon's habitability.

Poster #20

Quantification of Magnetosphere - Ionosphere coupling timescales using mutual information: response of terrestrial radio emissions and ionospheric/magnetospheric currents

Alexandra Ruth Fogg, C. M. Jackman, S. C. Chapman, J. E. Waters, A. Bergin, L. Lamy, K. Issautier, B. Cecconi, X. Bonnin

Auroral kilometric radiation (AKR) is the strongest terrestrial radio emission, and emanates from the same electron acceleration regions which excite the auroral ionosphere. Previous studies have indicated effects of upstream and substorm drivers on the morphology and intensity of AKR emission, although the exact relationship is yet to be determined, and appears to be non-linear. In this study, we use mutual information to assess the correlation between AKR intensity, determined from the Wind/WAVES instrument, and various geomagnetic indices at different temporal lags. This process enables quantification of a "peak" lag with the most shared information between time series, which can be interpreted as a coupling timescale between the two parameters. By exploiting geomagnetic indices derived from different latitudes, we quantify the coupling timescale between the AKR source region and different regions in the magnetosphere. We find that the polar ionosphere is excited before any corresponding AKR enhancement; the opposite is true for the auroral ionosphere. Finally, no strong relationship is found between AKR intensity and equatorial latitudes.

Poster #21

Variations of the peak positions in the longitudinal profile of noon -time equatorial electrojet

Zie, T.

In this study, the seasonal variations of the EEJ longitudinal profiles were examined based on the full CHAMP satellite magnetic measurements from 2001 to 2010. A total of 7537 satellite noon-time passes across the magnetic dip-equator were analyzed. On the average, the EEJ exhibits the wave-four longitudinal pattern with four maxima located, respectively, around 170° W, 80° W, 10° W and 100° E longitudes. However, a detailed analysis of the monthly averages yielded the classification of the longitudinal profiles in two types. Profiles with three main maxima located, respectively, around 150° W, 0° and 120° E, were observed in December solstice (D) of the Lloyd seasons. In addition, a secondary maximum observed near 90° W in November, December and January, reinforces from March to October to establish the wave-four patterns of the EEJ longitudinal variation. These wave-four patterns were divided into two groups: a group of transition which includes equinox months March, April and October and May in the June solstice; and another group of well-established wave-four pattern which covers June, July, August of the June solstice and the month of September in September equinox. For the first time, the motions in the course of seasons of various maxima of the EEJ noon-time longitudinal profiles have been clearly highlighted.

Poster #22

Constraints of ground-based detections of Uranian electrostatic discharges

Dualta Ó Fionnagáin, Aaron Golden, Jean-Mathias Griessmeier, Tobia Carrozzi, David McKenna

Most planetary bodies in the solar system are thought to produce lightning in their atmosphere. There has been one instance of a ground-based non-terrestrial lightning

detection in low frequency radio, in the case of Saturn using the UTR-2 telescope. The ability to detect these events from the ground would allow us to probe the atmospheres of these planets remotely, monitoring for meteorological activity. We present a monitoring campaign using NenuFAR and LOFAR to search for electrostatic discharges in the Uranian atmosphere between 15-60 MHz. The use of multiple stations allows for anti-coincidence flagging for RFI and other non-Uranian sources. Our observations can place constraints on either the frequency of these events, or the ability of these events to be detected by current ground-based radio telescopes.

Poster #23

The peak frequency source of Saturn's Kilometric Radiation

L. Lamy

Before to ultimately plunge into Saturn's atmosphere, the Cassini spacecraft explored between 2016 and 2017 the auroral regions of Saturn's magnetosphere, where rises the Saturn's Kilometric Radiation (SKR). This powerful, nonthermal, radio emission analog to Earth's Auroral Kilometric Radiation, is radiated through the Cyclotron Maser Instability (CMI) by mildly relativistic electrons at frequencies close to the local electron gyrofrequency. The typical SKR spectrum, which ranges from a few kHz to ~1MHz, thus corresponds to auroral magnetic flux tubes populated by radio sources at altitudes ranging from ~4 kronian radii (Rs) down to the planetary ionosphere. During the F-ring orbital sequence, Cassini probed the outer part of both northern and southern auroral regions, ranging from ~2.5 to ~4 Rs altitudes, and crossed several SKR low frequency sources (~10-30 kHz). Their analysis showed that the radio sources strongly vary with time and local time, with the lowest frequencies reached on the dawn sector. They were additionally colocated with the UV auroral oval and controlled by local time-variable magnetospheric electron densities, with important consequences for the use SKR low frequency extensions as a proxy of magnetospheric dynamics. Along the proximal orbits, Cassini then explored auroral altitudes below ~2.5 Rs and crossed numerous, deeper, SKR sources at frequencies close to, or within the emission peak frequency (~80-200 kHz). Here, we present preliminary results of their survey analysis, taking advantage of HST remote UV observations coordinated with Cassini in situ radio and magnetic measurements. Understanding how the CMI operates in the widely different environments of solar system magnetized planets has direct implications for the ongoing search of radio emissions from exoplanets, ultracool dwarves or stars.

Poster #24

Jupiter's Auroral Radio Emissions Observed by Cassini: Rotational Versus Solar Wind Control, and Components Identification

P. Zarka, F. P. Magalhães, M. S. Marques, C. K. Louis, E. Echer, L. Lamy, B. Cecconi, R. Prangé

Reanalyzing Cassini radio observations performed during Jupiter's flyby of 2000–2001, we study the internal (rotational) versus external (solar wind) control of Jupiter's radio emissions, from kilometer to decameter wavelengths, and the relations between the different auroral radio components. For that purpose, we build a database of the occurrence of Jovian auroral radio components bKOM, HOM, and DAM observed by Cassini, and then frequency-longitude stacked plots of the polarized intensity of these radio components. Comparing the results obtained inbound and outbound, as a function of the Observer's or Sun's longitude, we find that HOM & DAM are dominantly rotation-modulated (i.e., emitted from searchlight-like sources fixed in Jovian longitude), whereas bKOM is modulated more strongly by the solar wind than by the rotation (i.e., emitted from sources more active within a given Local Time sector). We propose a simple analytical description of these internal and external modulations and evaluate its main parameters (the amplitude of each control) for HOM + DAM and bKOM. Comparing Cassini and Nançay Decameter Array data, we find that HOM is primarily connected to the decameter emissions originating from the dusk sector of the Jovian magnetosphere. HOM and DAM components form a complex but stable pattern in the frequency-longitude plane. HOM also seems to be related to the “lesser arcs” identified by Voyager. bKOM consists of a main part above ~40 kHz in antiphase with HOM occurrence, and detached patches below ~80 kHz in phase with HOM. The frequency-longitude patterns formed by DAM, HOM and bKOM remain to be modeled.

Poster #25

Ubiquitous Jupiter fast drifting radio bursts reveal Alfvénic electron acceleration

Philippe Zarka, Emilie Mauduit, Laurent Lamy

The galilean moon Io is known to interact electrodynamically with Jupiter’s magnetic field and ionosphere via Alfvén waves, producing electromagnetic signatures detectable remotely: decameter-wave radio emission generated along the Io Flux Tube (IFT) and UV aurora at the IFT footprints prolongated by a ‘tail’ emission. These emissions are thought to be produced by electrons having sustained Alfvénic acceleration. Indirect signatures of this acceleration process are the transverse magnetic fluctuations and the broadband electron energy spectra observed in the IFT and more generally in Jupiter’s auroral regions. A more direct signature is provided by the discrete, fast-drifting, quasi-periodic decameter radio bursts (so-called S-bursts) identified to date only in relation with the Io-Jupiter interaction. S-bursts generation by Alfvén waves has been thoroughly modelled, from electron acceleration to radio emission growth rate. The S-bursts discreteness and quasi-periodicity were correctly reproduced, whereas their time-frequency drift results from the adiabatic motion of accelerated electrons along the IFT. Here we present the first detection of S-bursts related to the Ganymede-Jupiter interaction and to the main Jovian aurora, revealing thus the ubiquitous character of Alfvénic electron acceleration in Jupiter’s high-latitude regions. We estimate the Alfvén wave periods and the accelerated electrons energy in each case. Two populations of accelerated electrons are found to co-exist, with different energies (a few keV and a few hundred eV).

Instrumentation

Poster #26

NenuFAR, a new low-frequency radiotelescope for studying planetary, solar, exoplanetary and stellar radio emissions

P. Zarka and the NenuFAR-France collaboration

We present the characteristics of the new low-frequency radiotelescope NenuFAR, near completion in Nançay (France). It provides an exceptional sensitivity in the 10-85 MHz range, the lowest observable from the ground, and can be used in various modes: beamforming, imaging, waveform capture, LOFAR super station. After a ~3-year commissioning and Early Science period, it will be open to the international community for part of its observing time from December 1st, 2022. Observations programs can be proposed in response to semester calls, and will be selected as usual based on scientific merit and limited overlap with the ongoing Key Programs. We will also present a selection of the early results from NenuFAR on planetary, solar, exoplanetary and stellar radio emissions.

Poster #27

Thunderbolts and Lightning, very very enlightening: Engaging and educating audiences with public displays of a 1 million volt musical Tesla Coil.

Mark Langtry

Getting hit in the face with a million volts of lightning and living to tell the tale is not something we can all claim to have done. Dancing around in our room to rock 'n' roll is something we may have all done. But both together? Surely not? Explorium Science Centre in Dublin, is home to the world's first 'Lightning Room', where brilliant sparks of lightning zap around to the tune of your favourite songs. High frequency, high voltage alternating current pulses are controlled by a midi player, which turns thunder into musical notes. A faraday suit protects the presenter from the deadly bolts of lightning. Is there a better way to learn about one of nature's most dangerous and captivating phenomenon?

Poster #28

STELLAR: An EU Twinning Project on LOFAR Data Analysis and Knowledge Transfer

K. Kozarev, R. Miteva, A. Antonova, P. Zucca, E. Carley, P. Petkov, S. Maloney, R. Vermeulen, P. Gallagher, M. Dechev, P. Zhang, A. Avramova-Boncheva, A. Manolova, M. Nedal, M. Mevius, A. Mutafov, M. Iacobelli

The Scientific and Technological Excellence by Leveraging LOFAR Advancements in Radio Astronomy (STELLAR) is a project of mutual collaboration and know-how transfer in the field of radio astronomy (RA), solar physics and space weather using the Low Frequency Array (LOFAR) instrument and data. Two institutions from Bulgaria – the Institute of Astronomy and National Astronomical Observatory of the

Bulgarian Academy of Sciences (IANAO) and the Technical University-Sofia (TUS) – benefit from technical and scientific know-how exchange from world-leading RA institutions – ASTRON (the Netherlands) and DIAS (Ireland) – via a series of training hands-on sessions, workshops, seminars and project-focused schools for both students and senior staff. This effort is complementary to the development of a Bulgarian LOFAR-BG station. Here we present the activities of the STELLAR project, and the plan for LOFAR-BG. The STELLAR project is funded by the European Union's Horizon 2020 research and innovation programme under grant agreement No 952439. The LOFAR-BG project is funded by the Ministry of Science and Education of Bulgaria. Both are coordinated by IANAO.

Poster #29

The Radio JOVE Project 2.0

C. Higgins, S. Fung, L. Garcia, J. Thieman, J. Sky, D. Typinski, R. Flagg, J. Brown, F. Reyes, J. Gass, L. Dodd, T. Ashcraft, W. Greenman, J. Cox, and S. Blair

Radio JOVE is a well-known public outreach, education, and citizen science project using radio astronomy and a hands-on radio telescope for science inquiry and education. Radio JOVE 2.0 is a new direction using radio spectrographs to provide a path for radio enthusiasts to grow into citizen scientists capable of operating their own radio observatory and providing science-quality data to an archive. Radio JOVE 2.0 uses more capable software defined radios (SDRs) and spectrograph recording software as a low-cost ($350) radio spectrograph that can address more science questions related to heliophysics, planetary and space weather science, and radio wave propagation. Our goals are: (1) Increase participant access and expand an existing radio spectrograph network, (2) Test and develop radio spectrograph hardware and software, (3) Upgrade the science capability of the data archive, and (4) Develop training modules to help people become citizen scientists. We will overview Radio JOVE 2.0 and have a working radio spectrograph on display.

Poster #30

The Lunar Surface Electromagnetics Experiment: LuSEE 'Night'

Stuart D. Bale for the LuSEE team

The LuSEE-Night experiment is a payload selected for the NASA Commercial Lunar Payload Services (CLPS) program being implemented jointly by NASA and the US Department of Energy (DOE) and scheduled for deployment on a lunar lander in 2025. LuSEE-Night will be co-manifested with the ESA Lunar Pathfinder (LPF) relay satellite being developed by Surrey Satellite Technology Ltd (SSTL). LuSEE-Night will be deployed on the lunar farside and measure the radio and polarization spectrum from a few 100 kHz to 50 MHz over several lunar nights using a pair of crossed dipoles. To control system electromagnetic interference, the lander/spacecraft will shut down permanently and the LuSEE-Night system will operate on batteries with full frequency control. The payload will have its own S-band communication system and solar panels. LuSEE-Night will be a pathfinder for 21cm radio cosmology experiments on the Moon, making continuous full Stokes measurements through several lunar nights. LuSEE-Night should resolve the coronal blackbody spectrum and characterize the galactic synchrotron spectrum down to the free-free absorption trough at ~500 kHz. LuSEE-Night will measure nonthermal emission from the outer planets (when above the horizon) and, of course, solar radio bursts. Other discrete sources may become observable during the lunar nights. Another LuSEE payload, LuSEE 'Lite' will be deployed near the south pole Schroedinger Basin in 2024 and focus on lunar surface plasma physics.

Poster #31

SURROUND, A constellation of CubeSats around the Sun

L Alberto Canizares, Shane A Maloney, Peter T Gallagher, Eoin P Carley, Sophie Murray, Dale Weigt, Ciara McGrath, Nicholas Crisp, Alejandro Macario Rojas, Jack Cullen, Akhil Vinod Kumar

The Sun regularly produces coronal mass ejections (CMEs) and solar energetic particle events (SEPs) that can have a variety of adverse space weather (SW) effects at Earth and in the near-Earth environment. A useful means of tracking this activity is via solar radio bursts (SRBs); CME-driven shocks can be tracked via type II SRBs, while energetic electrons escaping into the heliosphere can be tracked via type III SRBs. Currently, there are no operational means to monitor and track SRBs throughout the inner heliosphere. SURROUND is a proposed constellation of CubeSats with the mission of observing SRBs in order to track CME and SEPs for SW monitoring. Each SURROUND satellite will be equipped with a radio spectrometer observing in the frequency range 0.01–25 MHz, enabling radio burst tracking from 2–150 solar radii. This mission concept is currently going through a Phase 0 study, supported by ESA. SURROUND will potentially be composed of 6 CubeSats; one at each of the Lagrange 1, 4 and 5 points, one orbiting ahead of the Earth, one orbiting behind the Earth, and one out of the ecliptic plane. This configuration would allow accurate three dimensional (3D) triangulation of SRBs and their associated SW activity. Our objective to routinely monitor and track solar radio bursts is complementary to the mission goals of ESA Solar Orbiter/RPW, NASA Parker Solar Probe/FIELDS and SunRISE, among other spacecraft. SURROUND will provide Europe with more accurate monitoring and forecasting of space weather activity in near real-time.

Poster #32

A consolidated catalogue of Jovian decametric radio emissions observed in Nançay from January 1978 to 1990

Baptiste Cecconi, Laura Debisschop, Laurent Lamy

A series of five Jovian decametric radio emission catalogues covering 13 years of observations (1978 to 1990) and published between 1981 and 1993 has been compiled after a digitisation process. The new catalogue has been validated and is provided in a standardised and interoperable format.

Poster #33

Daily observations of Jupiter and the Sun with the Nançay Decameter Array : long-term monitoring and support to space missions

L. Lamy, P. Zarka, B. Cecconi, A. Loh, A. Duchêne, E. Mauduit, L. Debisschop, C. Louis, S. Aicardi, C. Briand, N. Vilmer, S. Masson, S. Musset, G. Kenfack, P. Renaud, C. Viou, S. Barth, F. Jacquet, G. Auxepaules, H. Jacôme, M. Marques, E. Echer

Decametric observations of Jupiter’s magnetosphere (within 10-40 MHz) and of the solar corona (within 10-80+ MHz) are acquired quasi-daily by the Nançay Decameter Array since Jan. 1978. Hereafter, we will present recent efforts of the NDA team to

obtain high quality observations with digital receivers, to reformat the existing digital database (>1990) and make it compliant with VO (Virtual Observatory) tools, to digitize the decametric observations archived on analog devices (<1990) and to renew the electronics of the telescope to ensure perennial observations over the past decade and beyond, both in a stand-alone mode and as a support to space missions (such as Juno, JUICE, Parker Solar Probe and Solar Orbiter). We will also introduce recent results obtained from the analysis of NDA data for both Jupiter and the Sun.

Poster #34

Re-exploring the radio spectrum of Uranus with a novel orbital mission : science case and digital instrumentation

L. Lamy, B. Cecconi, M. Dekkali, P. Zarka, M. Moncuquet, C. Briand, F. Pantellini, L. Griton, X. Bonnin, P.-L. Astier, D. Dias, C. Louis

Among the known planetary magnetospheres, those of Uranus and Neptune display very similar radio environments so that they have early been referred to as ‘radio twins’. Their pioneer exploration by the Voyager 2 Planetary Radioastronomy experiment revealed a variety of electromagnetic radio waves ranging from ~0 to a few tens of MHz similar to - although more complex than - those of Saturn or the Earth. Nonetheless, the asymmetric magnetosphere of Uranus is unavoidably the most atypical with a large obliquity, magnetic tilt, and fast rotation period, so that the magnetosphere undergoes perpetual reconfiguration. In this contribution, we will review the various and complex Uranian radio emissions, including the auroral Uranian Kilometric Radiation (UKR) between a few 10kHz and 1 MHz, Uranian Electrostatic Discharges (UED) observed up to 40 MHz, and low frequency waves (continuum, whistler mode emissions) observed at few kHz. We will then present a modern concept of digital High Frequency Receiver (HFR) within the framework of a general Radio and Plasma Wave (RPW) experiment to be proposed to a future orbital mission toward Uranus. The presented HFR concept, based on the heritage of Cassini/RPWS/HFR, Bepi-Clompobo/PWI/Sorbet, Solar Orbiter/RPW and JUICE/RPWI/JENRAGE is aimed at providing a light, robust, low-consumption versatile instrument capable of goniopolarimetric and waveform measurements from a few kHz to ~20MHz, devoted to the study of auroral and atmospheric radio and plasma waves or dust impacts.

Exoplanets

Poster #35

Comparative visibility of planetary auroral radio emissions and implications for the search for exoplanets

L. Lamy, C. Louis, J. Waters

The powerful radio waves emanating from the auroral regions of the terrestrial and giant planet's magnetospheres are radiated at large angles from the local magnetic field vector (and sometimes further affected by refraction along the raypath) while being produced over spatial regions generally limited in altitude and local time/longitude. As a result, their final visibility strongly depends on the position of the observer. Understanding this visibility is therefore essential to assess the reliability of the diagnostic brought by remote radio observations of the planetary auroral and magnetospheric activities. This has been in turn a topic intensively studied, generally on a planet-by-planet basis. Here, we wish to compare those results on a solar system basis, taking advantage of recent statistical studies led at Earth, Jupiter and Saturn, and discuss implications for the search of exoplanetary auroral radio emissions.